Environmental Toxicology and Pharmacology 97 (2023) 104034

Contents lists available at ScienceDirect

Environmental Toxicology and Pharmacology

journal homepage: www.elsevier.com/locate/etap

BDE-99 (2,2′,4,4′,5 - pentain polybrominated diphenyl ether) induces toxic effects in *Oreochromis niloticus* after sub-chronic and oral exposure

Joelma Leão-Buchir [a,b], Tugstênio Lima de Souza [a], Claudemir de Souza [a], Luís Fernando Fávaro [a], Patrícia Manuitt Brito [a], Milena Carvalho Carneiro [c], Bruna Hilzendeger Marcon [d], Luíse Esquivel [e], Ciro Alberto de Oliveira Ribeiro [a], Maritana Mela Prodocimo [a,*]

[a] Departamento de Biologia Celular, Universidade Federal do Paraná, Curitiba, Brazil
[b] Departamento de Toxicologia Molecular e Ambiente, Centro de Biotecnologia, Universidade Eduardo Mondlane, Maputo, Mozambique
[c] Departamento de Imunologia, Instituto de Ciências Biomédicas, Universidade de São Paulo, São Paulo, Brazil
[d] Instituto Carlos Chagas, Fiocruz, Curitiba, Brazil
[e] Estação de Piscicultura Panamá, Paulo Lopes, Brazil

ARTICLE INFO

Edited by Dr. Alan Jeffrey Hargreaves

Keywords:
Water quality
Biomarkers
Brominated flame retardants
Freshwater
Tilapia

ABSTRACT

PBDEs are toxic, lipophilic, hydrophobic, and persistent artificial chemicals, characterized by high physical and chemical stability. Although PBDEs are known to disturb hormone signaling, many effects of 2,2′,4,4′,5 - pentain polybrominated diphenyl ethers (BDE-99) in fish remain unclear. The current study investigates the effects of BDE-99 in *Oreochromis niloticus* where sixty-four juvenile fish were orally exposed to 0.294, 2.94, 29.4 ng g^{-1} of BDE-99, every 10 days, during 80 days. The results showed histopathological findings in liver and kidney, increasing acetylcholinesterase activity in muscle, disturbs in the antioxidant system in liver and brain and decreasing the plasmatic levels of vitellogenin in females. According to multivariate analysis (IBR), the higher doses are related to the interaction of oxidative and non-oxidative enzymes. The present study provided evidence of deleterious effects after sub-chronic exposure of BDE 99 to *O. niloticus,* increasing the knowledge about its risk of exposure in fish.

1. Introduction

The demand for a modern society and increase of economic activity are responsible for an increase of electronic wastes around the world (Zhu et al., 2014; Chen et al., 2016); creating serious environmental problems, especially in developing countries (Chen et al., 2017). PBDEs (Polybrominated diphenyl ethers) are a class of flame retardants that were introduced in the 1970s, with levels increasing exponentially in the environment, wildlife, and humans (Thornton et al., 2016; Leão-Buchir et al., 2021). These compounds are highly lipophilic, environmentally persistent, and have the potential to bioaccumulation (Alonso et al., 2010; Yu et al., 2015; Chalifour and Tam, 2016; Díaz-Jaramillo et al., 2016; Arkoosh et al., 2017; Krieger et al., 2017; Lee et al., 2020; Li et al., 2020; Margolis et al., 2020; Montalbano et al., 2020; Pardo et al., 2020; Wu et al., 2020; Leão-Buchir et al., 2021). Commercial PBDEs are manufactured by bromination of diphenyl ethers resulting in a mixture of ethers containing tetra-, penta-, hepta-, octa-, and deca-congeners in various percentages. There are 209 possible congeners divided into 10 congener groups from mono- to deca-BDE, and BDE-99 is one of the most common, and widely detected in environmental, food and human samples (Zhao et al., 2014; Song et al., 2016; Thornton et al., 2016; Han et al., 2017; Mi et al., 2017; Liu et al., 2020; Montalbano et al., 2020).

PBDEs have potential adverse effects on aquatic life and humans, including effects on the thyroid system, endocrine disrupting effects, reproductive toxicity, liver toxicity, pancreas effects and neuro-development toxicity, however, date about exposure to BDE-99 are little discussed, mainly in fish (Benedict et al., 2007; Yuan et al., 2016; Farzana et al., 2017; Li et al., 2020). Exposure of zebrafish to BDE-99 led to developmental changes and disruption of thyroid (Zezza et al., 2019; Wu et al., 2020), while the studies conducted in larvae revealed neuro-behavioral disturbances (Margolis et al., 2020). PBDEs can trigger mechanisms of estrogenic/antiestrogenic activity in response to

* Correspondence to: Laboratório de Toxicologia Celular, Universidade Federal do Paraná, Caixa Postal 19031, CEP 81531-970 Curitiba, Brazil.
E-mail address: maritana.mela@gmail.com (M.M. Prodocimo).

https://doi.org/10.1016/j.etap.2022.104034
Received 27 December 2021; Received in revised form 27 October 2022; Accepted 4 December 2022
Available online 7 December 2022

estrogen signaling in hepatocytes (Yamamoto et al., 2017). Additionally, was reported that these compounds can induce cellular redox imbalance impairing the antioxidant defenses and so disrupting the biomolecules integrity (Margolis et al., 2020; Lee et al., 2020); while the physiological disorders are related to morphological damages in targeted organs (Gutteridge and Halliwell, 2000; Yamamoto et al., 2016; Wolf and Wheeler, 2018; Folle et al., 2020; Gemusse et al., 2021; Oliveira Ribeiro et al., 2022).

To evaluate the toxicity of chemical pollutants in aquatic organisms the use of different kinds of biomarkers is widely stimulated (Wolf and Wheeler, 2018). In an environmental context, biomarkers offer promise as sensitive indicators demonstrating that toxicants have entered organisms, have been distributed between tissues, and are eliciting a toxic effect at critical targets (Van der Oost et al., 2003). The use of biomarkers is considered extremely important because it allows the detection of sublethal effects on organisms, enabling preventive actions for the conservation of ecosystems (Calado et al., 2019).

Fish, specifically *Oreochromis niloticus* was recently used experimentally in studies to evaluate the effects of PBDEs (Folle et al., 2020; Leão-Buchir et al., 2021; Oliveira Ribeiro et al., 2022) or for biomonitoring of aquatic environments (Yamamoto et al., 2017; Gemusse et al., 2021; Rubio-Vargas et al., 2021). This species is widely distributed in the world, can persist in adverse habitats and is used as a biological monitor of environmental pollution (Carvalho et al., 2012; Moustafa et al., 2020). Thus, the main goal of the present study was to investigate experimentally the effects of exposure to BDE-99, after oral and sub chronic exposure considering a multibiomarker approach.

2. Materials and methods

2.1. Experimental design

Juvenile Nile tilapia (*O. niloticus)* were obtained at Panama Pisciculture Farm (Paulo Lopes city, Santa Catarina State, Brazil) (www.pisciculturapanama.com.br) and transported to the laboratory of Federal University of Paraná (UFPR). Fish were acclimated during 14 days, into tanks (150 L), with a flow-through system, controlled water conditions and fed twice a day with commercial pellets (Poytara®). These same conditions were adopted during the experiment. After acclimation period, sixty-four fish (59.64 g ± 19.08 and 12.79 cm ± 15.02) (mean ± standard deviation), among males and females, were distributed in 4 experimental groups in a total of 12 tanks 100 liters capacity each (15 fish in control group, and 18, 17, 14 fish in experimental groups 0.294, 2.94 and 29.4 ng. g^{-1} BDE-99, respectively). Each treatment was conducted in triplicate with at least 4 individuals per tested group. The differences in number observed among the experimental groups was necessary to maintain the groups as homogeneous as possible. The individuals were orally exposed every 10 days during 80 days, while the control group received only the vehicle corn oil. Fish exposure to BDE-99 was performed by gavage where the BDE-99 was initially prepared in DMSO and after diluted in corn oil, to obtain three stock solutions containing a final concentration of 14.700, 1.470 and 147 ngBDE-99/mL. Each animal received 2 μL of corn oil containing BDE-99 (tested groups) or only corn oil (control groups) per gram of weight to reach to a dose of 29.4, 2.94 and 0.294 ng. g^{-1} BDE-99, corresponding to a nominal dose of 3.675, 0.3675 and 0.03675 ng. g^{-1} BDE-99, respectively. The purity of BDE-99 was considered to prepare the stock solution. The experimental design was based on the studies reported by Arkoosh et al. (2017) and Kuo et al. (2010) considering the bioaccumulation of BDE-99 in fish muscle after environmental exposure, and in our more recent studies with brominated compounds (Folle et al., 2021, Leão-Buchir et al., 2021 and Oliveira Ribeiro et al., 2022).

All experimental procedures were approved by the Ethics Committee for the Use of Animals Experimentation (CEUA) Sciences Biological Sector from the Federal University of Parana (Protocol number 1200/2017).

2.2. Biological sampling

Ten days after the last gavage (80th day), the animals were anesthetized with MS222 (0.02 %) (Sigma/Aldrich®), and the blood was immediately sampled from the caudal vein following the morphometry determination as weight length body. The fish were then euthanized by the medullary section. The liver, kidney, gonads, brain and muscle were collected and preserved at − 80 °C for biochemical or molecular analysis, while kidney, liver and gonads samples were chemically preserved for histopathological studies. At the end of the experiment the fish presented the following weights and measures, respectively: 73.65 g ± 17.98/15.83 cm ± 1.57 (mean ± standard deviation).

2.3. Somatic biomarkers

The condition index (K) was calculated by the relationship between length and weight as follows: K = (fish weight/fish length^3) *100. The Hepatosomatic index (HSI) and gonadosomatic index (GSI) were determined by the following expressions: HSI = (liver wet weight/fish weigh) *100 and GSI = (gonad wet weight/fish weigh) *100 (Ríos et al., 2017).

2.4. Immunodetection of vitellogenin

2.4.1. Enzyme - Linked Immunoassay

Sandwich indirect assays were carried out in polystyrene microplate (Maxisorb; Nunc, Roskilde, Denmark), coated with 100 μL of capture anti-VTG antibody (0.2 μg/mL), diluted in coating buffer (50 mM bicarbonate/ carbonate pH 9.6) and incubated for 16 h at 4 °C. Nonspecific binding sites were blocked with 150 μL/well of the 2 % (w/v) bovine serum albumin (BSA) (Sigma- Aldrich) in PBS 1x for 90 min at room temperature. For positive control, 286 μg/mL tilapia VTG and purified induced male and non-induced EE2 male as a negative control, were added to the assay. Then, 100 μL diluted plasma samples (1:10) were incubated for 90 min at 37 °C. For primary detection, biotinylated anti-VTG (0.74 μg/mL) was diluted to 1 μg/mL and 100 μL/well of this solution were incubated for 60 min at 37 °C. The possible sample/antibodies interactions were detected by secondary antibody (100 μL of streptavidin-conjugated with HRP peroxidase - 1:10,000) for 1 h at room temperature. After each incubation step, the plates were washed three times with PBS-T. The color reaction was developed by substrate TMB (3,3′, 5,5-tetramethylbenzidine) for 20 min followed by the addition of 50 μL/well of 2 M H_2SO_4 to the reaction stop. The assay absorbance was measured in the Varioskan™ LUX Multimode Microplate Reader (Thermo Fisher Scientific) at 450 nm (Nagamatsu et al., 2020, with modifications).

2.4.2. Western blot assay

The reference parameter for choosing the samples for this analysis was the absorbance values of the male and female specimens of the control group found in the ELISA assay, being next to zero for males and next to 1.0 for females. Values highly distant from this were considered as a potential effect of the pollutant. Thereby, were selected two specimens of each sex and treatment presenting respective absorbance values of the majority specimens of each group. For this purpose, the *O. niloticus* plasma samples were diluted five times in Tris-buffered saline and total proteins were estimated by spectrophotometry at 280 nm in Varioskan™ LUX Multimode Microplate Reader (Thermo Fisher Scientific). So then, 30 μg/well of plasma proteins were previously separated through SDS-PAGE under reducing conditions with polyacrylamide 9 % 0.75 mm gels (Mini-PROTEAN® Tetra Vertical Electrophoresis systems – Bio-Rad) stained with Coomassie Brilliant Blue R250 for SDS-PAGE analysis or transferred to an Amersham™ Program® nitrocellulose membrane (Merck Millipore, Bedford, MA) for Western blot analysis, by Trans-Blot® SD Semi-Dry Transfer Cell (Bio-Rad) for 75 min at 20 volts. The membrane was blocked with 5 % (w/v) nonfat dry milk in Phosphate

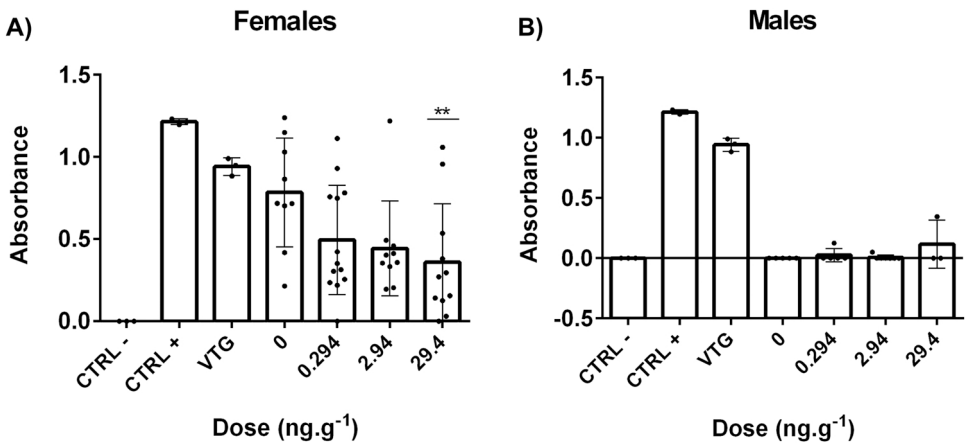

Fig. 1. Vitellogenin levels detected by ELISA in females (A) and males (B) plasma of *O. niloticus* exposed to BDE 99 (0.294, 2.94 and 29.4 ng. g^{-1}). ** Values differ significantly from the control group ($p < 0.01$). ANOVA one-way, Dunnet *post* test.

Buffered Saline with Tween-20 (0.1 %) for 60 min and after three washes were incubated with 0.6 μg. mL^{-1} of the rabbit polyclonal antibody generated for *O. niloticus* vitellogenin (Folle, 2018 – unpublished data) for 16 h at 4 °C followed by secondary incubation with Goat anti-Rabbit IgG Alkaline Phosphatase Conjugated (# T2191, Thermo Fisher Scientific) (1: 5000) for 60 min. The membrane reaction was revealed by BCIP/NBT Color Development Substrate (S3771, Promega) for 2 min (Nagamatsu et al., 2020, with modifications).

2.5. Biochemical biomarkers

The liver was homogenized in Tris-buffer (20 mM Tris-HCl, 1.0 mM EDTA, pH 7.6, 1 mM PMSF) while the brain and muscle were in potassium phosphate buffer (0.1 M, pH 7.5). The homogenate was centrifuged (20 min at 12,000 x g at 4 °C), the supernatants (10 μL) were recovered and mixed to Bradford reagent (250 μL) in a 96-well microplate, and absorbance was measured at 595 nm. A standard curve of bovine serum albumin was used to determine the total protein concentration (Bradford, 1976).

2.5.1. Catalase activity (CAT)

The supernatant (20 μL, 0.3 mg protein/mL) was mixed with 180 μL of reaction medium (20 mM H_2O_2, 50 mM Tris-base, 0.25 mM EDTA, pH 8.0) in a 96-well UV-star® microplate (Greiner Bio-One), and the absorbance decreased was immediately measured at 240 nm for 5 min. The molar extinction coefficient for H_2O_2 (40 $M^{-1}{\cdot}cm^{-1}$) was used to calculate catalase activity (Aebi, 1984, with modifications).

2.5.2. Superoxide dismutase activity (SOD)

Liver and brain supernatant (30 μL; 1.0 mg protein/mL) and 70 μL of 572 μM nitrotetrazolium blue chloride (NBT) in 0.1 mM EDTA were mixed in a 96-well microplate. For the reference curve, the supernatant was replaced by Tris-EDTA buffer (20 mM Tris-HCl, 1 mM EDTA, pH 7.4). The reaction was initiated by adding 100 μL of hydroxylamine chloride in 0.5 M sodium carbonate, pH 10.2. The reduction of NBT by $O2^{-}$ to blue formazan was measured as a constant increase of absorbance at 560 nm for 30 min (Kono, 1978).

2.5.3. Glutathione S-transferase activity (GST)

Liver and brain supernatant (20 μL; 1.0 mg protein/mL) were added to 96-well microplates, followed by the addition of reaction medium (180 μL, 1.5 mM GSH (glutathione), 2.0 mM 1-chloro-2,4-dinitrobenzene (CDNB), 0.1 M potassium phosphate buffer, pH 6.5. The absorbance increase was measured at 340 nm for 5 min and the molar extinction coefficient for CDNB (9.6 $mM^{-1}.cm^{-1}$) was used to calculate the GST activity (Keen et al., 1976).

2.5.4. Glutathione peroxidase activity (GPx)

Liver and brain supernatant (20 μL; 1.0 mg/mL protein) was added to a 96-well microplate. Two reaction media were used: the first was prepared in a sodium phosphate buffer (0.1 M, pH 7) containing sodium azide (2 mM), NADPH (0.2 mM), GSH (2 mM), and 45 μL of GR. The second medium contained sodium phosphate buffer (0.1 M, pH 7.0) and 0.5 mM hydrogen peroxide. First, 140 μL of the first reaction medium was added, followed by the addition of 40 μL of the second medium. The absorbance decrease was immediately measured at 340 nm for 5 min, and the GPx activity was calculated using the molar extinction coefficient for NADH (6.22 M^{-1} cm^{-1}) (Wendel, 1981).

2.5.5. Glutathione disulfide reductase activity (GR)

Liver and brain supernatant (50 μL; 1.0 mg/mL protein) was added in a 96-well microplate followed by 150 μL of the reaction medium (0.1 M potassium phosphate buffer, pH 7.6, 0.5 mM NADPH and 5.0 mM GSSG). The absorbance decrease was immediately measured at 340 nm for 5 min, and the GR activity was calculated using the molar extinction coefficient for NADH (6.22 M^{-1} cm^{-1}) (Sies et al., 1979).

2.5.6. Glucose-6-phosphate dehydrogenase activity (G6PDH)

Liver and brain supernatant (30 μL; 1.0 mg/mL protein) in homogenization buffer (20 mM Tris-HCl, 1.0 mM EDTA, pH 7.6, 1 mM PMSF) and white (Tris-EDTA) was pipetted in triplicate in 96-well plates. Then, 170 μL of the reaction medium was added to each well and the increase in absorbance was immediately measured at 340 nm. The increase in absorbance is caused by the reduction of NADP+ to NADPH by G6PDH (Glock and Mclean, 1953).

2.5.7. Non-protein thiols (NPT)

Liver and brain supernatant protein precipitated with 10 % trichloroacetic acid (TCA) and centrifuged (1000*g*, 4 °C, 15 min). A volume of 50 μL of supernatant was added into 96-well microplates, followed by 230 μL of 0.4 M Tris-based buffer, pH (8.9) and 20 μL of 2.5 mM DTNB. The absorbance was measured at 415 nm and NPT concentration was calculated based on a standard GHS curve (Sedlak and Lindsay, 1968).

2.5.8. Lipid peroxidation (LPO)

Liver and brain supernatant (200 μL) were mixed with 800 μL of the reaction medium (0.1 mM xylenol orange, 25 mM H_2SO_4, 4.0 mM butylated hydroxytoluene (BHT)) and 0.25 mM FeSO4. NH4 (ammonium ferrous sulfate) in 90 % methanol. After 20 min, centrifuge at 9.000 g for 10 min at room temperature, 200 μL of supernatant were pipetted into 96-well microplates, and absorbance was measured at 570 nm. The hydroperoxides concentration was calculated using the apparent molar extinction coefficient for H2O2 and cumene

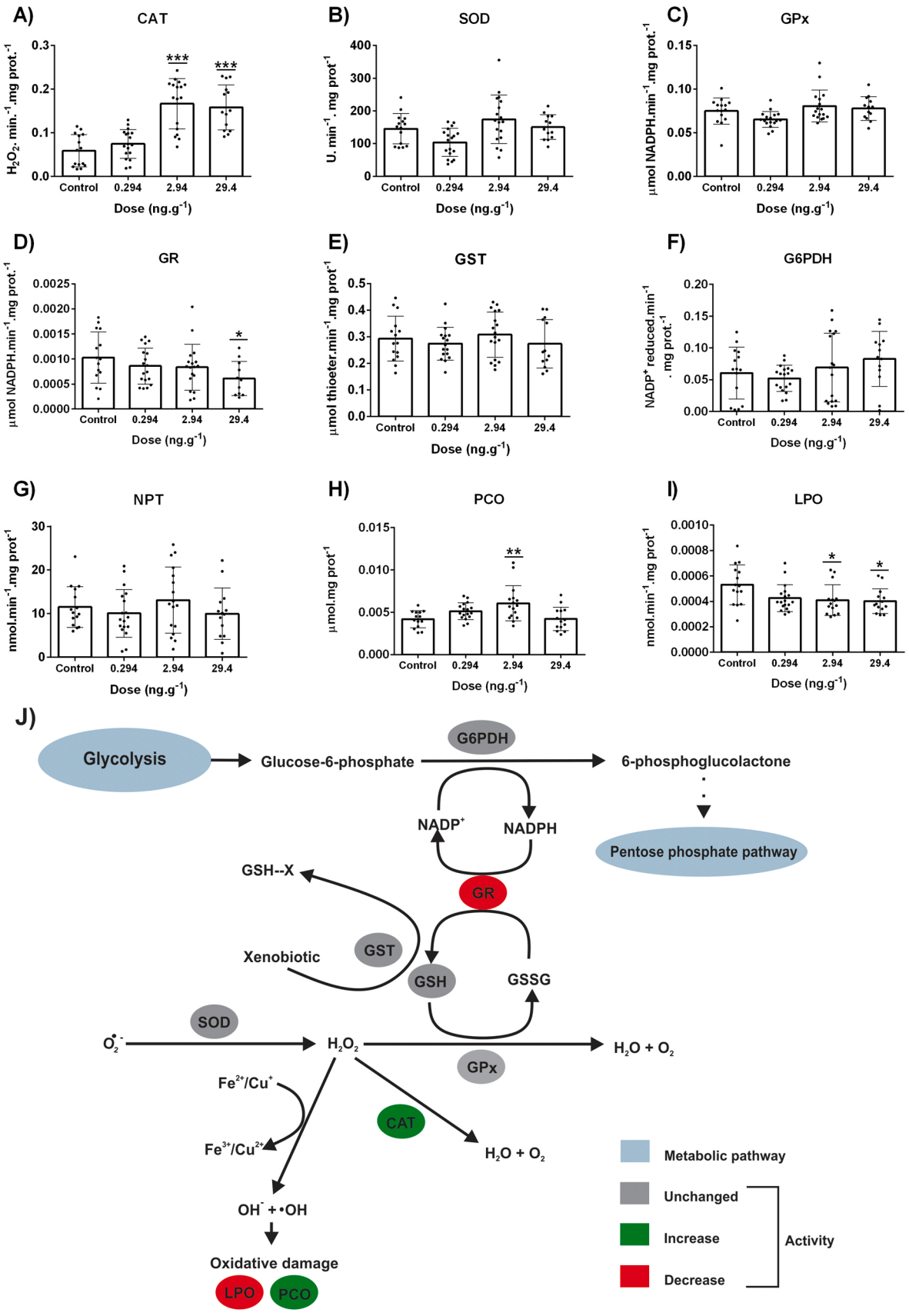

Fig. 2. Biochemical biomarkers of antioxidant mechanisms in the liver of *O. niloticus.* A) Catalase (CAT). B) Superoxide dismutase (SOD). C) Glutathione peroxidase (GPx). D) Glutathione disulfide reductase (GR). E) Glutathione S-transferase (GST). F) Glutathione-6-phosphate dehydrogenase (G6PDH). G) Non-protein thiols (NPT). H) Protein carbonylation (PCO). I) Lipid peroxidation (LPO). J) BDE-99 action on hepatic antioxidant system (Adapted from Souza et al. (2020)).*= $p < 0.05$; ** = $p < 0.01$; ***= $p < 0.001$ (ANOVA test *post hoc* Dunnet).

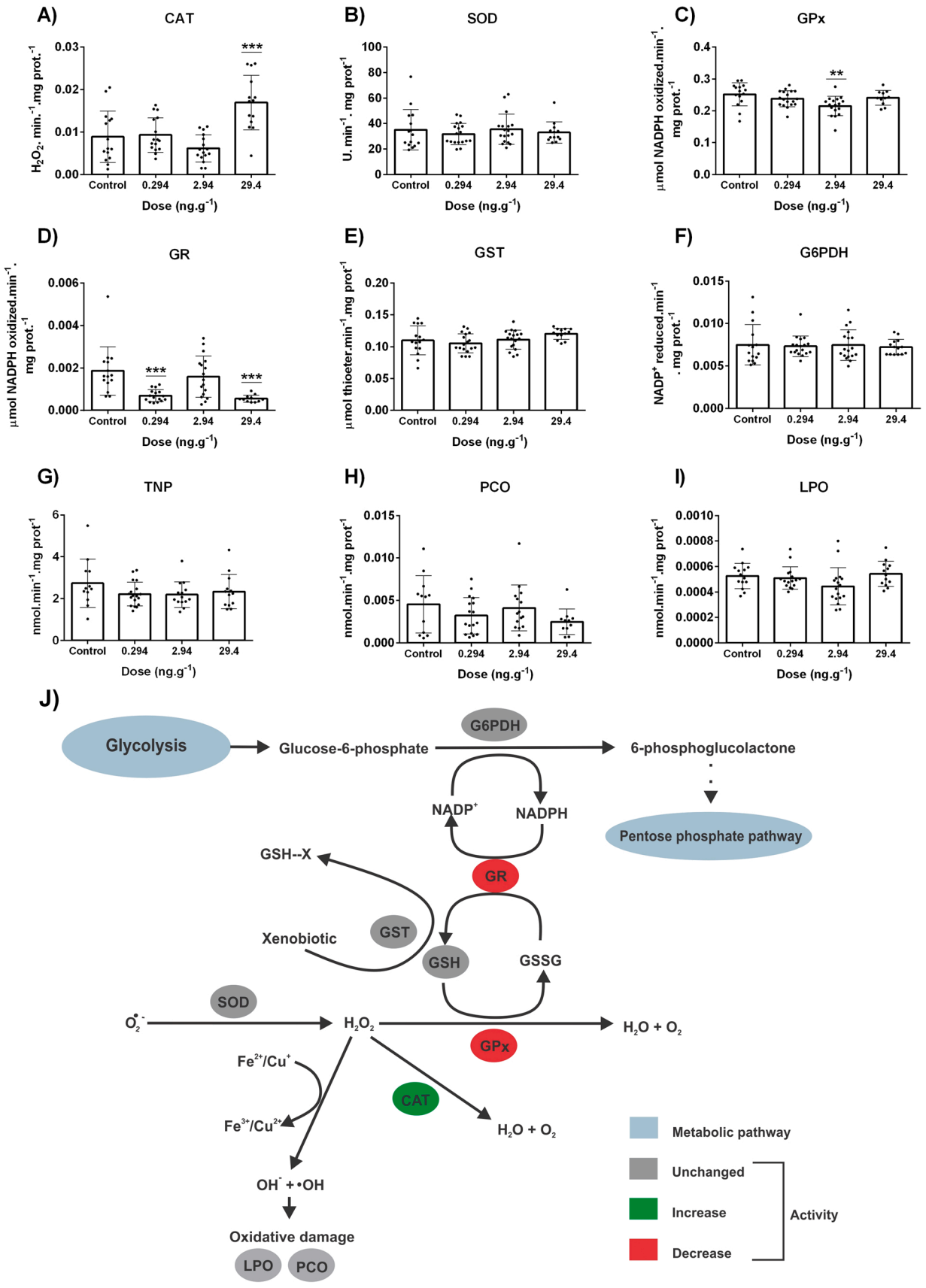

Fig. 3. Biochemical biomarkers and mechanism of oxidative stress induction in the brain of *O. niloticus*. A) Catalase (CAT). B) Superoxide dismutase (SOD). C) Glutathione peroxidase (GPx). D) Glutathione disulfide reductase (GR). E) Glutathione S-transferase (GST). F) Glutathione-6-phosphate dehydrogenase (G6PDH). G) Non-protein thiols (NPT). H) Protein carbonylation (PCO). I) Lipid peroxidation (LPO). J) BDE-99 action on brain antioxidant system (Adapted from Souza et al. (2020)). ** = $p < 0.01$; ***= $p < 0.001$ (ANOVA test *post hoc* Dunnet).

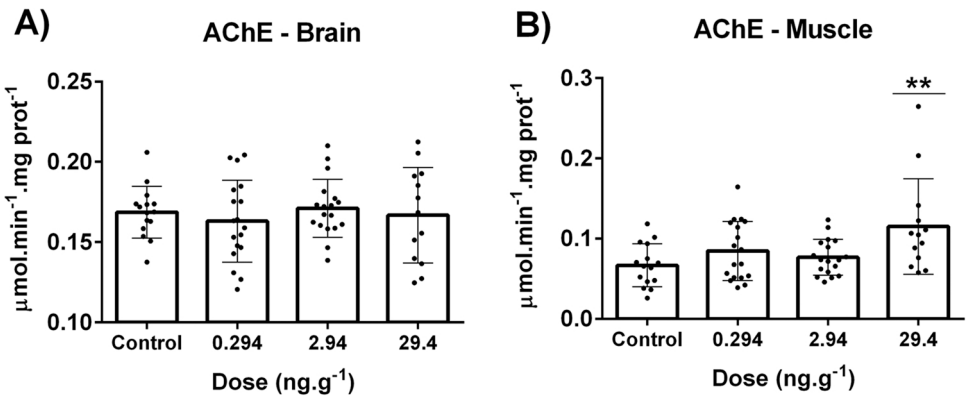

Fig. 4. Acetylcholinesterase activity (AChE) from *O. niloticus*. A) Brain; B) Muscle. ** = $p < 0.01$ (ANOVA - *post hoc* test: Dunnet).

hydroperoxide of 4.3×10^4 M^{-1} cm^{-1} (Jiang et al., 1992).

2.5.9. Protein carbonylation (PCO)

Liver and brain supernatant (200 µL; 2.0 mg/mL protein) were mixed with 500 µL of 10 mM 2,4-dinitrophenylhydrazine (DNPH) in 2 M HCl (test tube) and 2 M HCl (blank) and kept at 34 °C for 90 min. After incubation, 1 mL of 28 % trichloroacetic acid (TCA) was added. Pellet was resuspended with 1 mL of ethyl acetate/ethanol (1:1), mixed, and then centrifuge (9.000 g, 4 °C, 10 min). The pellet was resuspended in 500 µL of 6 M guanidine hydrochloride, centrifuged (9.000 g, 4 °C, 10 min). The supernatant (200 µL) was added to a 96-well microplate and absorbance reading at 360 nm. The molar extinction coefficient for hydrazone (2.1 ×104 M-1 cm-1) (Levine et al., 1994).

2.5.10. Acetylcholinesterase activity (AChE)

Muscle and brain supernatant (20 µL; 1.0 mg protein/mL) were added to a 96-well microplate followed by 130 µL of 0.75 mM DTNB in 0.1 M potassium phosphate buffer (pH 7.5). Then 50 µL of 9 mM acetylcholine iodide (in 0.1 M potassium phosphate buffer, pH 7.5) was added and the reading of absorbance was performed at 405 nm for 5 min. The molar extinction coefficient of 2-nitrobenzoate-5-mercaptothiocholine (13.6×10^3 M^{-1} cm^{-1}) was used to calculate the activity of AChE (Ellman et al., 1961).

2.6. Integrated response of biochemical biomarkers (IBR)

To evaluate the biochemical dynamics of biomarkers the methodology described by Beliaeff and Burgeot (2002) and modified by Sanchez et al. (2013) was applied to assess the integrated biomarker response (IBR). The biochemical results were divided by the corresponding control group and followed by logarithmized transformation to reduce the variance. From the log-transformed data (Yi), the mean (µ) and the standard deviation (sd) were calculated. The Yi values were standardized by the equation $Zi = (Yi-\mu)/sd$ to apply for each treatment and the difference between the treated and the control group (Z_i - Z_0) was used to define the deviation index of the biomarker (A). The results were plotted on a radar chart, where values above or below zero (control) indicate the stimulus or inhibition of a given biomarker. For the calculation of the IBR index of each group, the values of (A) were converted to absolute numbers (S) and summed.

2.7. Histopathological procedures

For light microscopy samples of liver, kidney and gonads were chemically preserved in ALFAC solution (70 % ethanol, 4 % formaldehyde, 5 % glacial acetic acid) for 16 h, washed in 70 % ethanol, dehydrated in graded ethanol concentrations and embedded in Paraplast® resin (Sigma) in a Micron Tissue Processor. Sagittal Section (5 mm thick) were obtained in Leica Microtome and stained with hematoxylin/eosin. The organ lesion index was calculated according to Bernet et al. (1999) modified by Mela et al. (2013). The lesions and alterations in tissue are classified in categories according to biological importance: 1 - minimal, easily reversible; 2 - moderate, reversible in most cases; and 3 - marked, generally irreversible, and severity establishing scores from 0 to 6. The organ lesion index for each group of lesions in liver or kidney was calculated using the formula: Iorg. = ∑rp ∑alt (a x w), where: *org* represents the organ (constant), *rp* is the reaction pattern, *alt* is the alteration, *a* represents the score value, and *w* is the importance factor of the lesion.

For ultrastructural analysis small pieces of liver were previously preserved in Karnovsky's solution (2,5 % glutaraldehyde, 4 % paraformaldehyde, 0.05 M sodium chloride in 0.1 M cacodylate, pH 7.4), at 4 °C for 2 h, washed in cacodylate buffer 0.1 M for 30 min, post-fixed in 2 % osmium tetroxide for 1 h and washed again in cacodylate buffer for 10 min (3 times). Posteriorly the samples were in block post-fixated with 0.2 % uranyl acetate for 2 h to increase membrane preservation and contrast in the images The specimens were then dehydrated in graded ethanol series (Merck), and embedded in PoliEmbed 812 DER736 resin (EMS) in a series of propylene oxide (EMS) and resin as follow: propylene oxide + resin (1:1), propylene oxide + resin (1:2) (2 h each) and pure resin (12 h under vacuum) (Mela et al., 2012). The ultrathin sections (70 nm thick) were obtained using a Leica Ultramicrotome, mounted on copper grids, contrasted with uranyl acetate water solution (20 min), lead citrate (5 min) and observed using a JEOL TEM-1400 Plus at 80 kV.

2.8. Statistical analysis

The data were tested for normality through the Kolmogorov-Smirnov test and homoscedasticity using the Barlett test and analyzed by one-way analysis of variance (ANOVA), followed by Dunnet *post hoc test*. All data were presented as mean ± standard deviation and p values < 0.05 were considered significant.

3. Results

3.1. Somatic characteristics

During the experiment no mortality was observed and somatic biomarkers did not reveal any physiological disturbs between treatments and the corresponding control groups (Supplementary Table).

3.2. Vitellogenin analysis

The ELISA assay showed that the levels of plasma VTG in females decreased in a dose-dependent way of BDE-99, what constitute evidence of antiestrogenic activity by exposure to the pollutant (Fig. 1A). However, in male fish, VTG was not detected in the control and exposed

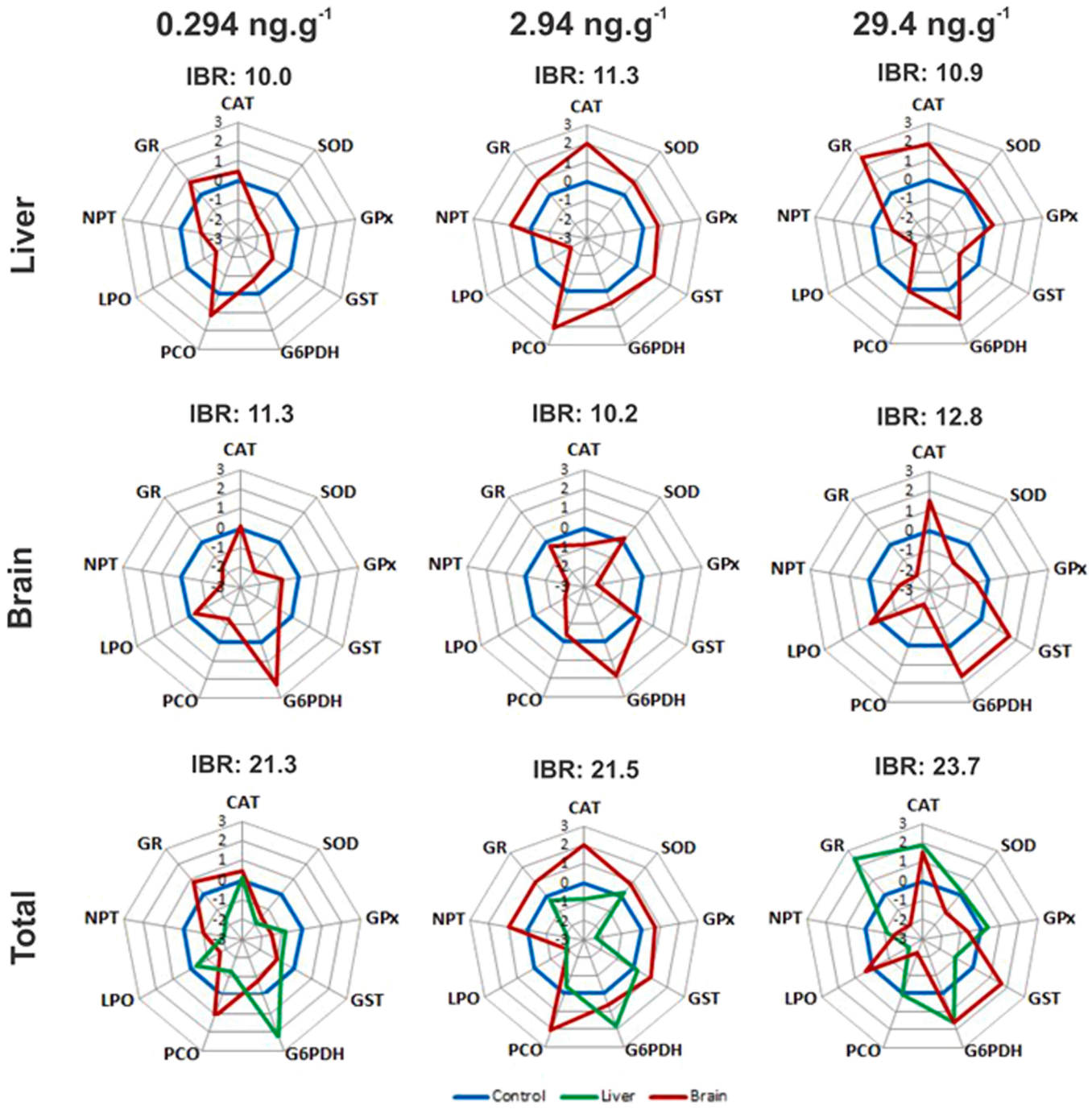

Fig. 5. Integrated biomarker response index of O. niloticus. Analyzed in the liver, brain and the interaction of both in CAT: Catalase; SOD: Superoxide dismutase; GPx: Glutathione peroxidase; GR: Glutathione disulfide reductase; GST: Glutathione S-transferase; G6PDH: Glutathione-6-phosphate dehydrogenase; NPT: Non-protein thiols; PCO: Protein carbonylation; LPO: Lipid peroxidation.

groups, indicating a non-estrogenic effect of BDE-99 (Fig. 1B).

SDS-PAGE stained with Coomassie Brilliant Blue showed that VTG consisted of a single band of approximately 200 kDa (Supplementary figure 1A-D). The western blot analysis confirmed detectable levels of VTG protein in plasma of females from the control group and exposed to 0.294 and 2.94 ng. g^{-1} of BDE-99 (Supplementary figure 2A-C). On the other hand, VTG was not detected on females exposed to 29.4 ng. g^{-1} of BDE-99 (Supplementary figure 2D). Similarly, to the ELISA results, the western blot did not detect VTG in males from the control group and those exposed to BDE-99.

3.3. Biochemical analysis

In the liver, the results showed an increase in the CAT activity in groups exposed to the higher doses of BDE-99 (2.94 ng. g^{-1} and 29.4 ng. g^{-1}) compared to the control group (Fig. 2A), but the same was not observed for SOD, GPx, GST and G6PDH enzymes (Fig. 2B, C, E and F). However, the activity of GR decreased significantly in individuals exposed to a higher dose (29.4 ng. g^{-1}) (Fig. 2D). From the non-enzymatic biochemical markers, the exposure to BDE-99 did not affect the level of NPT in liver (Fig. 2G) however, showed a significant increase in PCO levels after the exposure to intermediated dose (2. 94 ng. g^{-1}) (Fig. 3H) or a decrease in LPO levels in individuals exposed to the higher

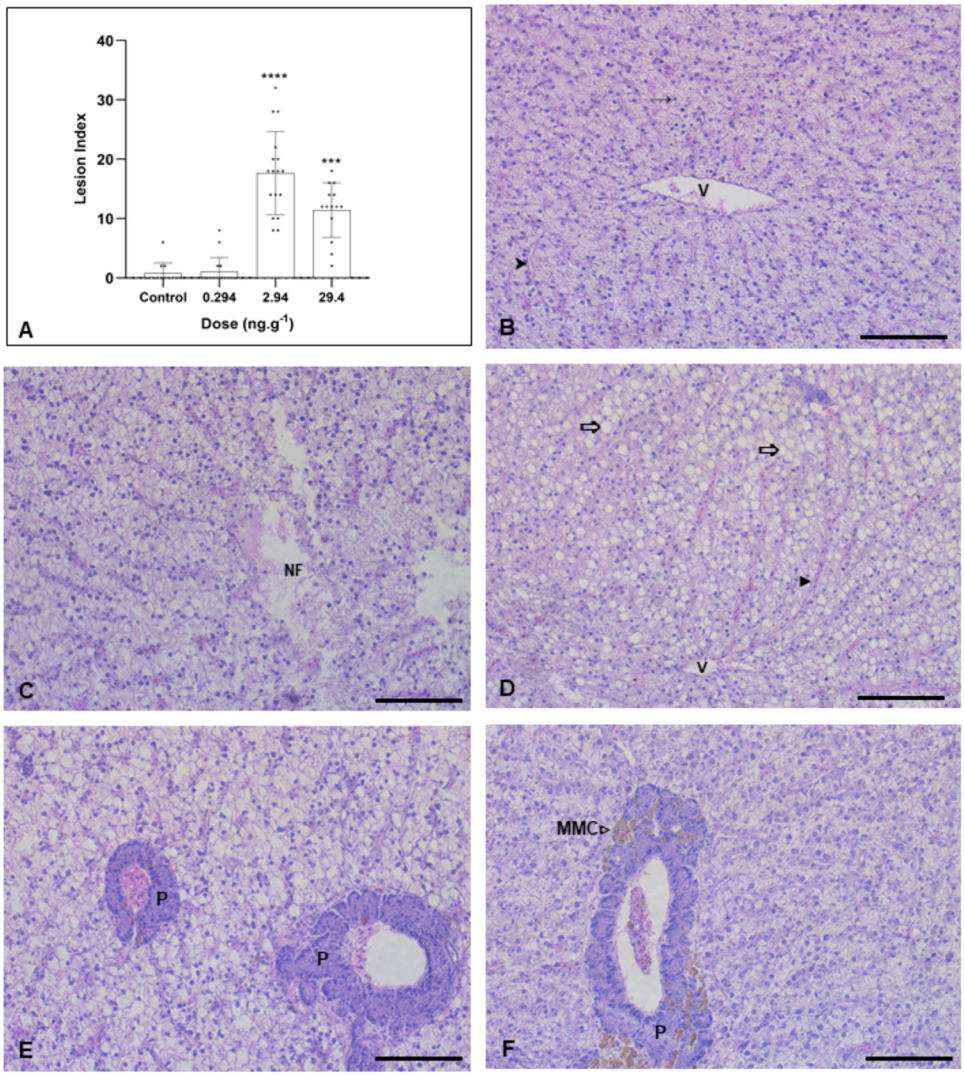

Fig. 6. Histological liver sections of O. niloticus counterstained with hematoxylin/eosin. A) Lesion index. ***= $p < 0.001$, **** = $p < 0.0001$. B) Liver of control group. Blood vessel (V), hepatocyte nuclei (→) and Sinusoid (>). C) Liver exposed group (2.94 ng. g-1). Necrotic foci (NF). D) Liver exposed group (29.4 ng. g-1). Blood vessel (V), Steatosis (→) and Hyperemia (▶). E) Liver of control group. Pancreatic tissue (P). F) Liver exposed group (2.94 ng. g-1). Melanomacrophages centers (↓↓MMC) associate to the Pancreatic tissue (P). Scale bars = 100 μm.

doses (2.94 ng. g^{-1} and 29.4 ng. g^{-1}) (Fig. 2I).

Results from the brain analysis revealed an increase in CAT activity in groups exposed to the higher dose (29.4 ng. g^{-1}) (Fig. 3A), but the opposite was found for the enzyme GPx in individuals exposed to intermediated dose (2.94 ng. g^{-1}) (Fig. 3C) and for GR activity in individuals exposed to the lower and higher doses (Fig. 3D). Other biomarkers such as SOD (Fig. 3B), GST (Fig. 3E) and G6PDH enzymes did not show significant changes (Fig. 3F). Contrary to the hepatic findings, BDE-99 did not affect the oxide reduction balance in the brain to the point of altering the levels of NPT, PCO, and LPO (Fig. 3G–I). Fig. 2J and 3J summarize the role of BDE-99 in the liver and brain of *O. niloticus*, after oral and subchronic exposure.

Evaluating the AChE activity, it was observed that there were no effects of BDE-99 on AChE activity in the brain (Fig. 4A), while in muscle, the brominated compound increased the AChE activity after subchronic exposure to the dose of 29.4 ng g^{-1} (Fig. 4B).

3.4. Integrated biomarker response (IBR)

Results of the IBR analysis from liver and brain considering the control and different treatments are shown in Fig. 5. The results showed that different treatments affected differently the target organs, where for liver BDE-99 is more toxic under intermediated dose (2.94 ng g^{-1}) while in brain the higher dose (29.4 ng g^{-1}) showed more effects. On the other hand, when the sum of the individual IBR results is analyzed, the result revealed that the biochemical disturbances are more evident in individuals exposed to the highest dose of BDE-99(IBR = 23.7).

3.5. Hepatotoxicity morphological and ultrastructural aspects

The liver parenchyma is organized by cells traversed by a network of sinusoids, where the polygonal hepatocytes are the most abundant cell type. In general, these cells show an uniform size, large rounded nuclei with prominent nucleoli and homogenous eosinophilic cytoplasm (Fig. 6B). The pancreatic tissue is found diffusely distributed in hepatic tissue with predominance of the exocrine portion, with acinar cells and oval nuclei (Fig. 6E). After the exposure to BDE-99 the occurrence of important histopathological findings was noted, namely, necrosis (Fig. 6C), hyperemia, steatosis (Fig. 6D) and infiltration of melanomacrophages in pancreatic tissue (Fig. 6F), where the lesion index for liver showed an increased effect in individuals exposed to the higher doses, comparatively with the control group (Fig. 6A). The liver ultrastructure confirmed the normal liver arrangement, showing the entire preserved structure (Fig. 7A). Hepatocytes have a well-developed rough endoplasmic reticulum, central spherical nucleus and a prominent nucleolus. Numerous circular or elongated mitochondria are distributed throughout the cytoplasm (Fig. 7B). The bile ducts are lined by a cuboidal epithelium (Fig. 7C). In pancreatic tissue it was possible to visualize zymogen granules (Fig. 7D). Hepatocytes, joined by tight junctions and desmosomes, originate small circular bile canaliculus.

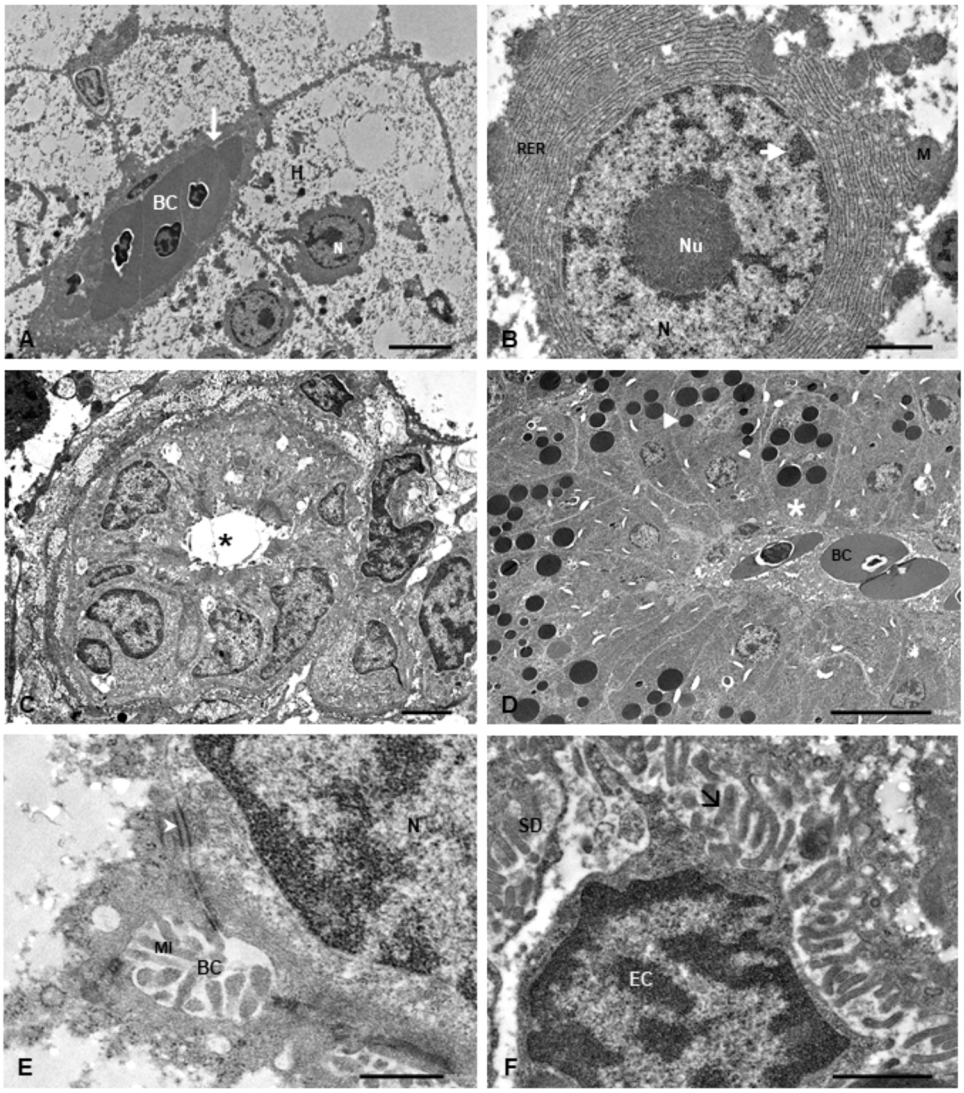

Fig. 7. Liver ultrastructure of O. niloticus under control conditions. A) Note the normal structure of the hepatic parenchyma. Polygonal hepatocyte (H), nucleus (N), lobular center vein (↓) with aggregations of red blood cells (BC). Scale bar: 5.0 μm. B) Hepatocyte nucleus with spherical appearance (N), Nucleoli (Nu), heterochromatin (▷), mitochondria scattered in the cytoplasm (M) and a well-developed rough endoplasmic reticulum (RER) arranged in parallel stacks at the lateral border of the nucleus. Scale bar: 1.0 μm. C) Bile duct (*) with epithelial cells, surrounded by connective tissue. Scale bar: 2.0 μm. D) Pancreatic acinar cells (*) with rounded nucleus in the basal portion and zymogen granules concentrated apically (▶). The Pancreatic tissue involves a vessel filled with red blood cells (BC). Scale bar: 10.0 μm. E) Hepatocytes join each other by tight junctions, the desmosomes (⧫), nucleus (N) and bile canaliculus originating by adjacent hepatocytes (BC). Note the microvilli (MI) filling the biliary canaliculus. Scale bar: 500.0 nm. F) Space of Disse (SD). Note the hepatocyte microvilli (▷) and the nuclei of endothelial cell (EC). Scale bar: 1.0 μm.

From the apical membrane long microvilli arise and fill lumen that become very narrow (Fig. 7E). The space of Disse, also called perisinusoidal space, the microvilli originating from hepatocytes are present (Fig. 7F). After the exposure to BDE-99, ultrastructural observations showed evident cell damages. In the cytoplasm lipid droplets of different sizes are observed distributed in clusters and surrounded by abundant glycogen rosettes (Fig. 8A). The hepatocyte nuclei showed difference in nuclear shape and disorganized and fragmented cisternae of RER were clearly recognized (Fig. 8B). Areas of necrosis accompanied by loss of cell limits were frequently observed, leading to changes in the integrity of the natural arrangement of hepatocytes (Fig. 8C). Myelin figures of various sizes and shapes are cell debris detected in areas of abundant necrotic cells (Fig. 8D) as well in the space of Disse (Fig. 8E). In the space of Disse degenerations of hepatocytes microvilli were frequently observed (Fig. 8F). A schematic drawing of the ultrastructural damages in hepatocytes is shown in Fig. 9.

3.6. Kidney histopathology

The results of histological analysis of the kidney showed normal morphology in the control group, with prominent glomerulus, proximal and distal tubules (Fig. 10B), Corpuscles of Stannius (CS), small rounded or oval endocrine glands associated with the mesonephros, as found in teleost fish (Fig. 10C). However, after exposure to BDE-99 the kidney showed necrosis areas (Fig. 10D), hemorrhage sites (Fig. 10E), pyknotic nucleus, accumulation of adipose tissue and incidence of melanomacrophage centers (Fig. 10F). The lesion index in the renal tissue was higher in individuals exposed to the higher doses (2.94 ng. g^{-1} and 29.4 ng. g^{-1}) (Fig. 10A). The histological analysis of gonads did not reveal damages or expressive alteration in the tissue.

4. Discussion

In the present study we evaluated the effects of BDE-99 on *Oreochromis niloticus* to trophically exposed to environmental doses. The results showed that BDE-99 can cause morphological damages in liver and kidney, oxidative stress in liver and brain, neurotoxicity, and endocrine disruption and, all these changes induce physiological disturbances affecting reproduction, liver metabolism, detoxification, osmoregulation and behavior. The reallocation of energy for detoxifying mechanisms or even to cover the physiological disturbances depletes the reserves originally intended for growth (Liebel et al., 2013; Leão-Buchir et al., 2021). The condition factor (K) is used as an indication of the health status in fish and can be used to assess the exposure to pollutants (Ríos et al., 2017; Baudou et al., 2019). The current findings showed no variation in the K in fish exposed to BDE-99, also described by Ameur et al. (2015) in fish from a lagoon impacted by PBDEs and Folle et al. (2020) after oral and subchronic exposure to 2,4,6-Tribromofenol (TBP).

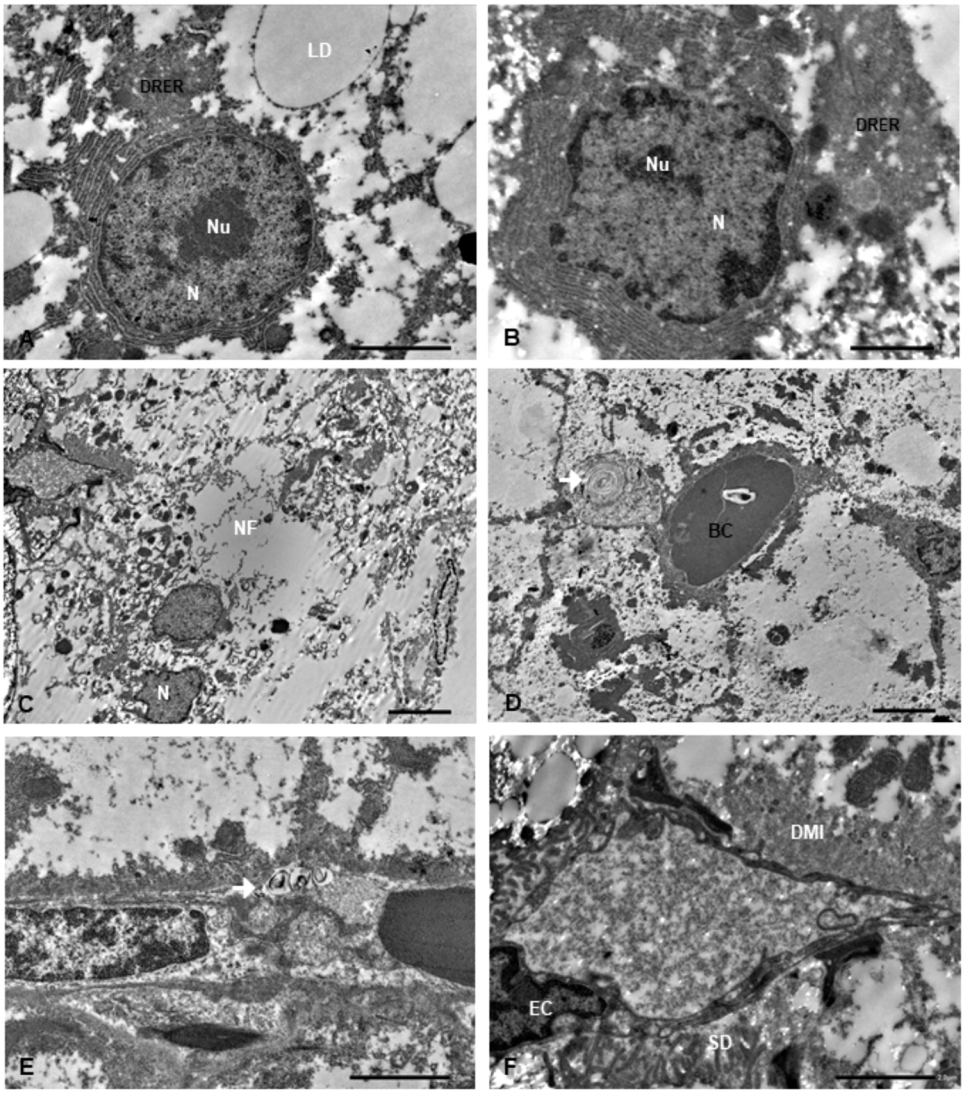

Fig. 8. Ultrastructure of liver in O. niloticus after exposure to BDE-99. A) Liver of exposed group (0.294 ng. g-1). Presence of lipid droplet (LD) and degenerated rough endoplasmic reticulum (DRER). The nucleus (N) and nucleolus (Nu) are preserved. Scale bar: 2.0 μm. B) Liver of exposed group (29.4 ng. g-1). Degenerated rough endoplasmic reticulum (DRER) and deformation of the nuclear outline (N) are observed. Nucleolus (Nu). Scale bar: 1.0 μm. C) Liver of exposed group (29.4 ng. g-1). Observe the Necrotic foci (NF) and deformation of the nuclear outline (N). Scale bar: 5.0 μm. D) Liver of exposed group (29.4 ng. g-1). Observed a central vessel, with red blood cells (BC), disintegration of hepatocytes limits and myelin figures (▷). Scale bar: 5.0 μm. E) Liver of exposed group (2.94 ng. g-1). Space of Disse (SD) with myelin figures (). Scale bar: 2.0 μm. F) Liver of exposed group (2.94 ng. g-1). Space of Disse (SD) lined by endothelial cells (EC). Note the degenerations of microvilli of hepatocytes (DMI). Scale bar: 2.0 μm.

According to Liebel et al. (2013), no changes were observed in condition factor from individuals collected in two impacted lakes in Brazil, suggesting that this species is physiologically more adapted to tolerate chemical impacts. The absence of effects on the GSI corroborate with the histological results found in gonads, and were also previously described to the species exposed to BDE-47 (Leão-Buchir et al., 2021). Although the same authors did not observe disturbances in the expression of vitellogenin in males after exposure to BDE-47 and BDE-99, these results differed from females exposed to BDE-99, which showed an anti-estrogenic effect. This finding suggests a potential endocrine disruption of BDE-99 in female O. niloticus, not observed in BDE-47 under the same experimental design. Therefore, BDE-99 acts as an anti-estrogenic agent. The BDE-99 hole partially corroborates the results described by Folle et al. (2020), in *O. niloticus* after exposure to TBP in a similar experimental condition. Interesting data showed that brominated compounds can disrupt the VTG production, but also suggest that this effect is strictly dependent on the brome position. According to Folle et al. (2020), a high rate of liver damages could impair the yolk protein precursor (VTG) and it explains the low levels of protein. Therefore, the liver alterations observed in the current study may also probably explain the antiestrogenic hole of BDE-99.

The current study showed that BDE-99 is not an endocrine disruptor for males, but develops an antiestrogenic hole in females after exposure to 29.4 ng. g^{-1} of BDE-99. These findings are in accordance with the one reported by Leão-Buchir et al. (2021) in same species of fish exposed to BDE-47. According to Yamamoto et al. (2017), most studies investigating exposure to pollutants described as endocrine disruptors in fish have used the VTG dosage as a consolidated biomarker in fish. This information is precisely related with reproduction, by interfering directly in the quality and quantity of eggs and, finally, in the viability of the produced embryos (Adeogun et al., 2016). In ecotoxicological studies, an important challenge is to connect the experimental results with risk for population maintenance and so the fish biodiversity. In this way, the disturbances of VTG levels when detected in female fish or even males, indicate a relevant reproductive biomarker in different levels of biological organization (Yamamoto et al., 2016). Although Teta and Naik (2017) described that the exposure of fish to chemical estrogens lead to adverse impact on the development of gonads, the current results showed that only the damage in gonads is not enough to identify reproductive effects in fish.

The AChE controls the levels of neurotransmitter in synaptic gap of cholinergic synapses and neuromuscular junctions of vertebrates, degrading the acetylcholine (Ach) in choline and acetic acid (Mela et al., 2013; Xie et al., 2014; Dey et al., 2016). An imbalance in ACh hydrolysis interferes with cholinergic neurotransmission, causing hyperstimulation of nicotinic and muscarinic receptors and consequent interruption of neurotransmission (Serafini et al., 2019). In relation to our study, the increase in muscle activity is an indicative of the fish's attempt to

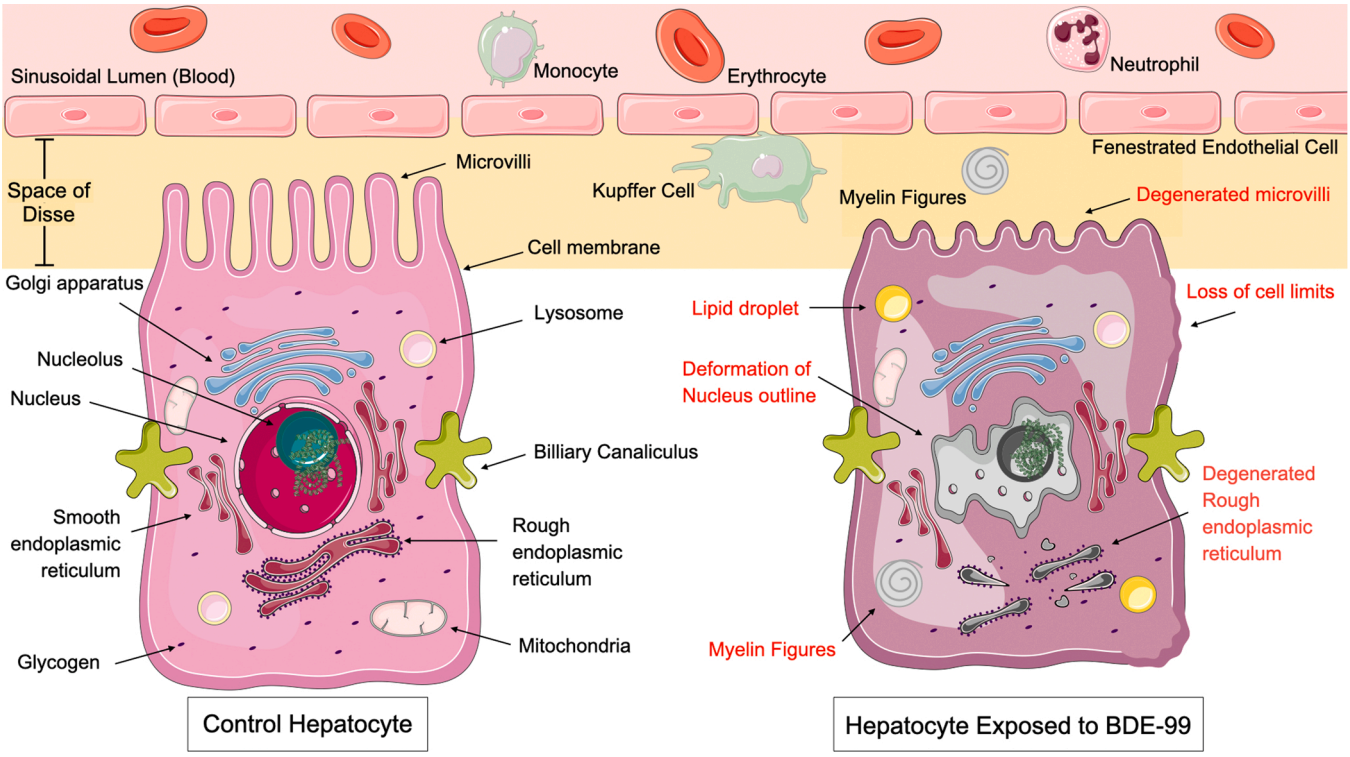

Fig. 9. Drawing of the hepatocyte architecture and schematic of the ultrastructural changes. This sketch represents a single hepatocyte flanked by bile canaliculus and one sinusoid, representing the apical and lateral membranes of the hepatocyte, respectively. Left: Hepatocyte of control fish. Hepatocyte nuclei round with prominent nucleoli. Abundant rough endoplasmic reticulum, smooth endoplasmic reticulum, mitochondria, Golgi apparatus, glycogen and lysosomes are observed. The endothelial cells of the liver sinusoids are fenestra. The hepatocytes have many microvilli which project into the space of Disse. A portion of the lateral faces of hepatocytes is modified to form bile canaliculus, containing microvilli, of two adjacent hepatocytes. Right: Hepatocyte after exposure to BDE-99. Presence of lipid droplet, degeneration of rough endoplasmic reticulum, deformation of the nuclear outline, loss of cell limits, presence of myelin figures and degenerations of hepatocyte microvilli. This figure was created using Servier Medical Art, licensed under a Creative Commons Attribution 3.0 Unported License: https://smart.servier.com. Color and structure adaptations from the original art were made on: hepatocytes, rough endoplasmic reticulum and nucleus.

compensate the stress caused by BDE-99. These results are in agreement with our recent study, in which exposure to BDE-47 produced similar enhanced effects on the muscular AChE activity of *O. niloticus* (Leão-Buchir et al., 2021). However, the increase in activity can influence the cholinergic neurotransmission process that induce lipid peroxidation levels. Similar results were also observed by Dey et al. (2016) in studies carried out with teleost fish exposed to glyphosate herbicide and Folle at al. (2020) in *O. niloticus* exposed to 2,4,6-Tribromophenol.

In both the liver and brain, it was observed that the absence of alteration in SOD activity may be explained by an increase in CAT activity, or the decrease in GPx that was only registered in the brain. These enzymes are involved in the process of preventing oxidative damage by eliminating hydrogen peroxide and its potential conversion to a hydroxyl radical (Lowe et al., 2012; Souza et al., 2019). These findings showed that BDE-99 can induce oxidative stress in both organs but is not enough to disrupt the antioxidant mechanism function, corroborated by absence of alteration in LPO levels in the brain as well as reducing its levels in the liver. These results showed that in the presence of other pollutants the exposure to BDE-99 can favor a pro-oxidant effect. The fact that the GPx in the liver has not changed may explain the elevated PCO levels observed in this tissue. However, with increased CAT activity, the H_2O_2 detoxification process can be supplied, leading to the increase of the capacity to eliminate reactive oxygen species (EROD). Similar results have been reported by Ghosh et al. (2013), in studies involving exposure of *Trematomus bernacchii* to the mixture of 8 PBDEs congeners.

GST activity, an important phase II enzyme involved in the metabolism of xenobiotics, was not significantly affected in both the liver and the brain. According to Souza et al. (2020), this enzyme uses reduced glutathione, a non-protein thiol (GSH) as a co-factor to make toxic metabolites more soluble and easily excreted by the kidney. Since the levels of NPT were not affected in the liver and brain, it explains that this mechanism was not activated to avoid injuries in hepatic tissues. This result is in line with the one reported by Folle et al. (2020) where alterations in these enzymes were not observed in tilapia exposed to TBP. The reduction in the activity of hepatic and cerebral GR, an enzyme responsible for catalyzing the reduction of GSSG in GSH, used by GPx or GST, is related to the decrease in cellular levels of NADPH, due to the low metabolic activity of glucose-6-phosphate dehydrogenase, and responsible for recycling NADP+ generated by GR activity, in NADPH. In the liver and brain, G6PDH activity was not significantly affected. This explains the non-alteration of the levels of NPT, with no need to reestablish them and consequently did not interfere in the activity of GST and GPx. Furthermore, the analysis of the IBR in biochemical biomarkers confirms the relevance in determining the dynamics of the redox action in the presence of BDE-99. However, the IBR values demonstrated that the action of enzymatic and non-enzymatic markers of oxidative stress in the studied organs is affected by the different doses used. Therefore, when sum the indexes of both organs for each treatment, it was observed that these organs are impacted by biochemical parameters variation when fish are exposed to highest dose of BDE-99, corroborating with studies conducted by Perussolo et al. (2019) and Souza et al. (2020).

The alterations observed in the liver, such as vascular congestion, reflect circulatory disturbance. Necrosis is related to increased levels of lipid peroxidation and reflects irreversible structural and functional damage (Mela et al., 2013; Freitas et al., 2020), and this kind of damage depending on the extension leads to the organ failure with no

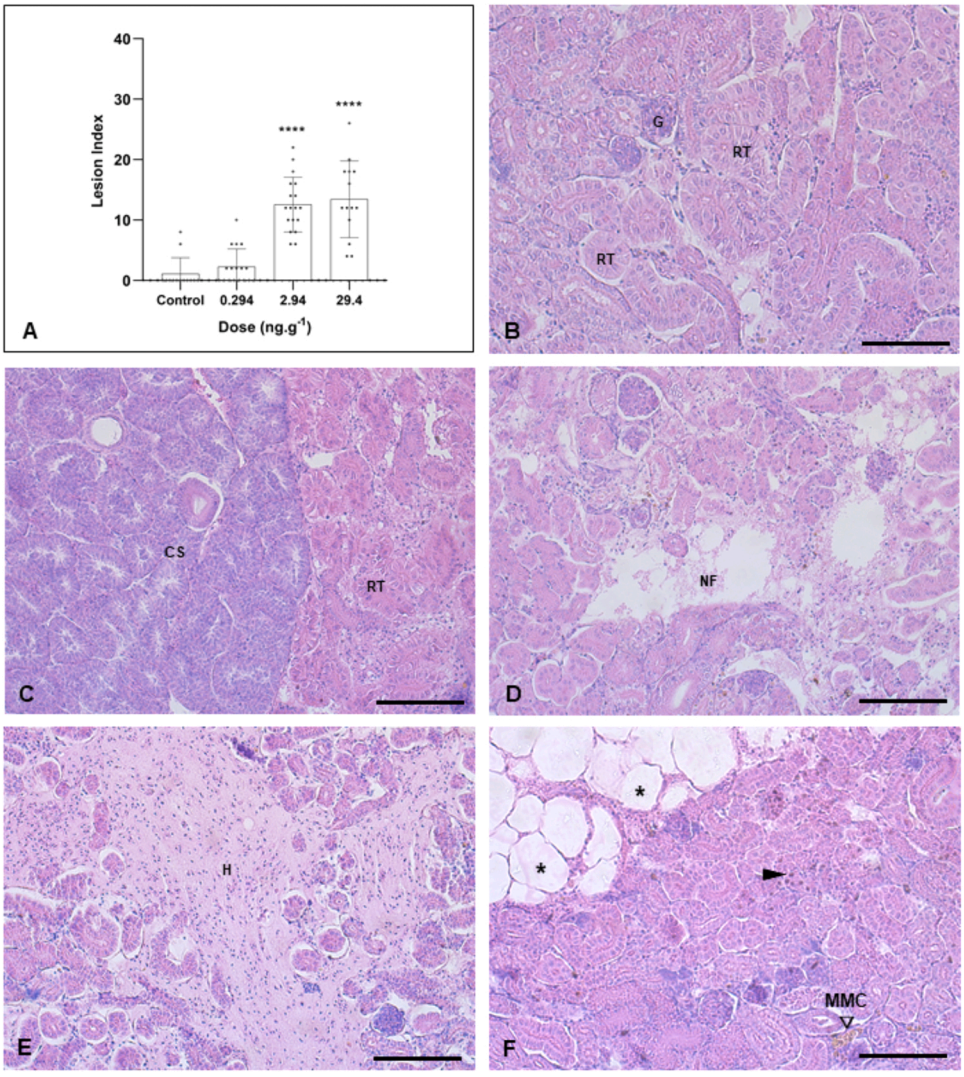

Fig. 10. Histological kidney sections of *O. niloticus* counterstained with hematoxylin/eosin. A) Lesion index. *** = $p < 0.001$, **** = $p < 0.0001$. B) Kidney of control group. Renal parenchyma filled with renal tubules (RT) and Glomerulus (G). C) Kidney of control group. Corpuscle of Stannius (CS) and renal tubules (RT). D) Kidney exposed group (29.4 ng. g-1). Necrotic foci (NF). E) Kidney of exposed group (2.94 ng. g-1). Hemorrhage (H). F) Kidney of exposed group (2.94 ng. g-1). Melanomacrophages centers (MMC), adipose tissue (*) and pycnotic nuclei (▶). Scale bars = 100 μm.

predictable physiological disturbs, explaining the presence of steatosis as alteration on hepatic metabolism. The presence of melanomacrophage centers is indicative of an inflammatory response to detoxification of xenobiotics (Mela et al., 2013) and are also linked with the damages as necrosis. The histopathological changes in the liver reported in the present study corroborate with the hepatic effects of BDE-47 in *Psetta maxima* described by Barja-Fernández et al. (2013) and of BDE-47, 99 e 209 in zebrafish (Zezza et al., 2019). In general, necrosis can be explained by the occurrence of oxidative stress (Zezza et al., 2019). The hepatic metabolism is a vital process when xenobiotics competes with endogenous compounds, what may also disrupt the endocrine system (Yang and Chan, 2015). The high liver lesion index observed in the treated groups when compared to the control group suggests that the BDE-99 caused morphological damages, which may result in tissue failure. The ultrastructural data confirmed in detail the changes in the liver evidenced by light microscopy.

The presence of pycnotic nuclei was observed in kidney, and can result from the oxidative stress and DNA damage, a process of migration of blood leukocytes to the renal tissue. Interstitial hemorrhage has also been observed and this disorder suggests impairment in the vascular process (Perussolo et al., 2019). The Kidney plays an important role in metabolism, osmoregulation and excretion of toxic compounds (Perussolo et al., 2019). The organ lesion index confirmed the toxicity of BDE-99 by the presence of leukocyte infiltration and MMC, characteristic of inflammatory response processes that in general are indicative of cell death and necrosis (Salgado et al., 2019). Similar findings were reported by Zhou et al. (2020) in a study conducting with *Oncorhynchus mykiss* after exposure to BDE-47. According to Folle et al. (2021), the occurrence of hemorrhage is an indicative of systemic disorders. The disturbance in lipidic metabolism is associated with the presence of adipose tissue (Mela et al., 2013) and pyknotic nucleus may be related to necrotic areas, alteration that was observed in the present study and corroborate by other (Fernandez et al., 2011; Wolf and Wheeler, 2018; Perussolo et al., 2019).

Overall, the current study showed that in ecotoxicological studies the use of multiple biomarkers is essential to understand the potential toxicity of pollutants in fish.

5. Conclusion

The present study demonstrated that environmentally relevant doses of BDE-99 are toxic to *O. niloticus* after oral and subchronic exposure. According to the results, the disturbances observed in components of the antioxidant system from the liver may explain the morphological damages in hepatic tissue and hepatocytes. Certainly, the severity of these effects could be the reason for disturbances in the VTG synthesis leading to reproductive failure, showing that BDE-99 acts as an endocrine disruptor in animals exposed to higher dose. These findings are in accordance with other brominated compounds toxicity, but particularly BDE-99 is an anti-estrogenic agent, cytotoxic and neurotoxic. In addition, the

current study confirms that a multibiomarkers approach represents a robust and accurate strategy to fully assess the environmental effects of pollutants on fish health.

Funding

This work was supported by the Coordination for the Improvement of Higher Education Personnel (CAPES, finance code 001) and Brazilian Conseils for Science and Technology – CNPq (Finance code 303118/2017-2).

CRediT authorship contribution statement

All authors worked equally and contributed to the final manuscript: BDE-99 (2,2′,4,4′,5 – pentain polybrominated diphenyl ether) induces toxic effects in Oreochromis niloticus: an emerging and dangerous contaminant.

Declaration of Competing Interest

The authors declare that they have no known competing financial interests or personal relationships that could have appeared to influence the work reported in this paper.

Data Availability

Data will be made available on request.

Acknowledgments and funding

The authors are grateful to Professor Marco Randi, Yuri Gonçalves, Roberta Pozzan, Aliciane Roque, Jessica Luz, Tobias Moraes and Luiza Barreto for assistance with fish maintenance and technical support during the experiments. We thank the Program for Technological Development in Tools for Health-PDTIS-FIOCRUZ for the use of the core facilities for microscopy (RPT07C).

Appendix A. Supporting information

Supplementary data associated with this article can be found in the online version at doi:10.1016/j.etap.2022.104034.

References

Adeogun, A.O., Onibonoje, K., Ibor, O.R., Omiwole, R.A., Chukwuka, A.V., Ugwumba, A. O., Ugwumba, A.A.A., Arukwe, A., 2016. Endocrine-disruptor molecular responses, occurrence of intersex and gonado-histopathological changes in tilapia species from a tropical freshwater dam (Awba Dam) in Ibadan, Nigeria. Aquat. Toxicol. 174, 10–21. https://doi.org/10.1016/j.aquatox.2016.02.002.

Aebi, H., 1984. [13] catalase in vitro. Methods Enzymol. 105 (C), 121–126. https://doi.org/10.1016/S0076-6879(84)05016-3.

Alonso, V., Linares, V., Bellés, M., Albina, M.L., Pujol, A., Domingo, J.L., Sánchez, D.J., 2010. Effects of BDE-99 on hormone homeostasis and biochemical parameters in adult male rats. Food Chem. Toxicol. 48, 2206–2211. https://doi.org/10.1016/j.fct.2010.05.048.

Ameur, W.Ben, El Megdiche, Y., de Lapuente, J., Barhoumi, B., Trabelsi, S., Ennaceur, S., Camps, L., Serret, J., Ramos-López, D., Gonzalez-Linares, J., Touil, S., Driss, M.R., Borràs, M., 2015. Oxidative stress, genotoxicity and histopathology biomarker responses in *Mugil cephalus* and *Dicentrarchus labrax* gill exposed to persistent pollutants. A field study in the Bizerte Lagoon: Tunisia. Chemosphere 135, 67–74. https://doi.org/10.1016/j.chemosphere.2015.02.050.

Arkoosh, M.R., Van Gaest, A.L., Strickland, S.A., Hutchinson, G.P., Krupkin, A.B., Dietrich, J.P., 2017. Alteration of thyroid hormone concentrations in juvenile Chinook salmon (*Oncorhynchus tshawytscha*) exposed to polybrominated diphenyl ethers, BDE-47 and BDE-99. Chemosphere 171, 1–8. https://doi.org/10.1016/j.chemosphere.2016.12.035.

Barja-Fernández, S., Míguez, J.M., Álvarez-Otero, R., 2013. Histopathological effects of 2,2′,4,4′-tetrabromodiphenyl ether (BDE-47) in the gills, intestine and liver of turbot (*Psetta maxima*). Ecotoxicol. Environ. Saf. 95, 60–68. https://doi.org/10.1016/j.ecoenv.2013.05.028.

Baudou, F.G., Ossana, N.A., Castañé, P.M., Mastrángelo, M.M., González Núñez, A.A., Palacio, M.J., Ferrari, L., 2019. Use of integrated biomarker indexes for assessing the impact of receiving waters on a native neotropical teleost fish. Sci. Total Environ. 650, 1779–1786. https://doi.org/10.1016/j.scitotenv.2018.09.342.

Beliaeff, B., Burgeot, T., 2002. Integrated biomarker response: a useful tool for ecological risk assessment. Environ. Toxicol. Chem. 21 (6), 1316–1322. https://doi.org/10.1002/etc.5620210629.

Benedict, R.T., Stapleton, H.M., Letcher, R.J., Mitchelmore, C.L., 2007. Debromination of polybrominated diphenyl ether-99 (BDE-99) in carp (*Cyprinus carpio*) microflora and microsomes. Chemosphere 69 (6), 987–993. https://doi.org/10.1016/j.chemosphere.2007.05.010.

Bernet, D., Schmidt, H., Meier, W., Burkhardt-Holm, P., Wahli, T., Kueng, C., Segner, H., Dutra, F.M., Rï¿½nnau, M., Sponchiado, D., Forneck, S.C., Freire, C.A., Ballester, E.L. C., Kipfer, S., Segner, H., Wenger, M., Wahli, T., Bernet, D., Luzio, A., Cáceres-Vélez, P.R., 1999. Histopathology in fish: proposal for a protocol to assess aquatic pollution. J. Fish Dis. 22, 25–34. https://doi.org/10.3354/dao061137.

Bradford, M.M., 1976. A rapid and sensitive method for the quantitation of microgram quantities of protein utilizing the principle of protein-dye binding. Anal. Biochem. 72 (1–2), 248–254. https://doi.org/10.1016/0003-2697(76)90527-3.

Calado, S.L.M., Vicentini, M., Santos, G.S., Pelanda, A., Santos, H., Coral, L.A., Magalhães, V.F., Mela, M., Cestari, M.M., Assis, H.C.S., 2019. Sublethal effects of microcystin-LR in the exposure and depuration time in a neotropical fish: Multibiomarker approach (2019). Ecotoxicol. Environ. Saf. 183, 109527 https://doi.org/10.1016/j.ecoenv.2019.109527.

Carvalho, C., dos, S., Bernusso, V.A., Araújo, H.S.S., de, Espíndola, E.L.G., Fernandes, M. N., 2012. Biomarker responses as indication of contaminant effects in *Oreochromis niloticus*. Chemosphere 89 (1), 60–69. https://doi.org/10.1016/j.chemosphere.2012.04.013.

Chalifour, A., Tam, N.F.Y., 2016. Tolerance of cyanobacteria to the toxicity of BDE-47 and their removal ability. Chemosphere 164, 451–461. https://doi.org/10.1016/j.chemosphere.2016.08.109.

Chen, L., Zhu, B., Guo, Y., Xu, T., Lee, J.-S., Qian, P.-Y., Zhou, B., 2016. High-throughput transcriptome sequencing reveals the combined effects of key e-waste contaminants, decabromodiphenyl ether (BDE- 209) and lead, in zebrafish larvae. Environ. Pollut. 214, 324–333. https://doi.org/10.1016/j.envpol.2016.04.040.

Chen, L., Wang, X., Zhang, X., Lam, P.K.S., Guo, Y., Lam, J.C.W., Zhou, B., 2017. Transgenerational endocrine disruption and neurotoxicity in zebrafish larvae after parental exposure to binary mixtures of decabromodiphenyl ether (BDE-209) and lead. Environ. Pollut. 230, 96–106. https://doi.org/10.1016/j.envpol.2017.06.053.

Dey, S., Samanta, P., Pal, S., Mukherjee, A.K., Kole, D., Ghosh, A.R., 2016. Integrative assessment of biomarker responses in teleostean fishes exposed to glyphosate-based herbicide (Excel Mera 71). Emerg. Contam. 2 (4), 191–203. https://doi.org/10.1016/j.emcon.2016.12.002.

Díaz-Jaramillo, M., Miglioranza, K.S.B., Gonzalez, M., Barón, E., Monserrat, J.M., Eljarrat, E., Barceló, D., 2016. Uptake, metabolism and sub-lethal effects of BDE-47 in two estuarine invertebrates with different trophic positions. Environ. Pollut. 213, 608–617. https://doi.org/10.1016/j.envpol.2016.03.009.

Ellman, G.L., Courtney, K.D., Andres, V., Featherstone, R.M., 1961. A new and rapid colorimetric determination of acetylcholinesterase activity. Biochem. Pharmacol. 7 (2), 88–95. https://doi.org/10.1016/0006-2952(61)90145-9.

Farzana, S., Chen, J., Pan, Y., Wong, Y., Shan, Tam, N.F.Y., 2017. Antioxidative response of Kandelia obovata, a true mangrove species, to polybrominated diphenyl ethers (BDE-99 and BDE-209) during germination and early growth. Mar. Pollut. Bull. 124 (2), 1063–1070. https://doi.org/10.1016/j.marpolbul.2016.12.041.

Fernandez, W.S., Dias, J.F., Ribeiro, C.A.O., Azevedo, J. de S., 2011. Liver damages and nuclear abnormalities in erythrocytes of *Atherinella brasiliensis* (Actynopterigii, Atherinopsidade) from two beaches in southeast of Brazil. Braz. J. Oceanogr. 59 (2), 163–169. https://doi.org/10.1590/S1679-87592011000200005.

Folle, N.M.T., Azevedo-Linhares, M., Garcia, J.R.E., Esquivel, L., Grotzner, S.R., Oliveira, E.C., de, Filipak Neto, F., Oliveira Ribeiro, C.A. de, 2020. 2,4,6-Tribromophenol is toxic to *Oreochromis niloticus* (Linnaeus, 1758) after trophic and subchronic exposure. Chemosphere 2020, 128785. https://doi.org/10.1016/j.chemosphere.2020.128785.

Folle, N.M.T., Azevedo-Linhares, M., Esquivel, J.R.G., Esquivel, L., Grotzner, S.R., de Oliveira, E.C., Filipak Neto, F., Oliveira Ribeiro, C.A., 2021. 2,4,6-Tribromophenol is toxic to Oreochromis niloticus (Linnaeus, 1758) after trophic and subchronic exposure. Chemosphere 268, 128785. https://doi.org/10.1016/j.chemosphere.2020.128785.

Freitas, J.S., Pereira, T.S.B., Boscolo, C.N.P., Garcia, M.N., Oliveira Ribeiro, C.A., Almeida, E.A., 2020. Oxidative stress, biotransformation enzymes and histopathological alterations in Nile tilapia (Oreochromis niloticus) exposed to new and used automotive lubricant oil. Comp. Biochem. Physiol. Part C: Toxicol. Pharmacol. 234. https://doi.org/10.1016/j.cbpc.2020.108770.

Gemusse, S.L., Folle, N.M.T., da Costa Souza, A.T., Azevedo-Linhares, M., Filipak Neto, F., Ortolani-Machado, C.F., Esquivel Garcia, J., Esquivel, L., da Silva, C.P., de Campos, S.X., de Castro Martins, C., Oliveira Ribeiro, C.A., 2021. Micropollutants impair the survival of *Oreochromis niloticus* and threat local species from Iguaçu River, Southern of Brazil. Environ. Toxicol. Pharmacol. 83 https://doi.org/10.1016/j.etap.2021.103596.

Ghosh, R., Lokman, P.M., Lamare, M.D., Metcalf, V.J., Burritt, D.J., Davison, W., Hageman, K.J., 2013. Changes in physiological responses of an Antarctic fish, the emerald rock cod (*Trematomus bernacchii*), following exposure to polybrominated diphenyl ethers (PBDEs). Aquat. Toxicol. 128–129, 91–100. https://doi.org/10.1016/j.aquatox.2012.11.019.

Glock, G.M., Mclean, P., 1953. Further studies on the properties and assay of glucose 6–phosphate dehydrogenase and 6-phosphogluconate dehydrogenase of rat liver. Biochem. J. 55, 400–408.

Gutteridge, J.M., Halliwell, B., 2000. Free radicals and antioxidants in the year 2000. A historical look to the future. Ann. N. Y. Acad. Sci. 899, 136–147.
Han, Z., Li, Y., Zhang, S., Song, N., Xu, H., Dang, Y., Liu, C., Giesy, J.P., Yu, H., 2017. Prenatal transfer of decabromodiphenyl ether (BDE-209) results in disruption of the thyroid system and developmental toxicity in zebrafish offspring. Aquat. Toxicol. 190, 46–52. https://doi.org/10.1016/j.aquatox.2017.06.020.
Jiang, Z.Y., Hunt, J.V., Wolff, S.P., 1992. Ferrous ion oxidation in the presence of xylenol orange for detection of lipid hydroperoxide in low density lipoprotein. Anal. Biochem. 202 (2), 384–389. https://doi.org/10.1016/0003-2697(92)90122-N.
Keen, J.H., Habig, W.H., Jakoby, W.B., 1976. Mechanism for the several activities of the glutathione S transferases. J. Biol. Chem. 251 (20), 6183–6188. https://doi.org/10.1016/S0021-9258(20)81842-0.
Kono, Y., 1978. Generation of superoxide radical during autoxidation of Hydroxylamine and an assay for superoxide-dismutase. Arch. Biochem. Biophys. 186, 189–195. https://doi.org/10.1016/0003-9861(78)90479-4.
Krieger, L.K., Szeitz, A., Bandiera, S.M., 2017. Hepatic microsomal metabolism of BDE-47 and BDE-99 by lesser snow geese and Japanese quail. Chemosphere 182, 559–566. https://doi.org/10.1016/j.chemosphere.2017.05.027.
Kuo, Y.-M., Sepúlveda, M.S., Hua, I., Ochoa-Acuña, H.G., Sutton, T.M., 2010. Bioaccumulation and biomagnification of polybrominated diphenyl ethers in a food web of Lake Michigan. Ecotoxicology 19, 623–634.
Leão-Buchir, J., Folle, N.M.T., Souza, T.L., Brito, P.M., Oliveira, E.C., Roque, A.A., Ramsdorf, W.A., Fávaro, L.F., Garcia, J.R.E., Esquivel, L., Neto, F.F., Oliveira Ribeiro, C.A., Prodocimo, M.M., 2021. Effects of trophic 2, 2′,4,4′-tetrabromodiphenyl ether (BDE-47) exposure in Oreochromis niloticus: a multiple biomarkers analysis. Environ. Toxicol. Pharmacol. 87, 103693 https://doi.org/10.1016/j.etap.2021.103693.
Lee, H.K., Kang, H., Lee, S., Kim, S., Choi, K., Moon, H.B., 2020. Human exposure to legacy and emerging flame retardants in indoor dust: a multiple-exposure assessment of PBDEs. Sci. Total Environ. 719, 137386 https://doi.org/10.1016/j.scitotenv.2020.137386.
Levine, R.L., Williams, J.A., Stadtman, E.P., Shacter, E., 1994. Carbonyl assays for determination of oxidatively modified proteins. Methods Enzymol. 233 (C), 346–357. https://doi.org/10.1016/S0076-6879(94)33040-9.
Li, J.B., Li, Y.Y., Shen, Y.P., Zhu, M., Li, X.H., Qin, Z.F., 2020. 2,2′,4,4′-tetrabromodipheny ether (BDE-47) disrupts gonadal development of the Africa clawed frog (*Xenopus laevis*). Aquat. Toxicol. 221 (February), 105441 https://doi.org/10.1016/j.aquatox.2020.105441.
Liebel, S., Tomotake, M.E.M., Oliveira Ribeiro, C., 2013. Fish histopathology as biomarker to evaluate water quality. Ecotoxicol. Environ. Contam. 8, 09–15.
Liu, Y., Feng, Y., Li, J., Zhou, D., Guo, R., Ji, R., Chen, J., 2020. The bioaccumulation, elimination, and trophic transfer of BDE-47 in the aquatic food chain of Chlorella pyrenoidosa-*Daphnia magna*. Environ. Pollut. 258, 113720 https://doi.org/10.1016/j.envpol.2019.113720.
Lowe, J., Souza-Menezes, J., Freire, D.S., Mattos, L.J., Castiglione, R.C., Barbosa, C.M.L., Santiago, L., Ferrão, F.M., Cardoso, L.H.D., da Silva, R.T., Vieira-Beiral, H.J., Vieyra, A., Morales, M.M., Azevedo, S.M.F.O., Soares, R.M., 2012. Single sublethal dose of microcystin-LR is responsible for different alterations in biochemical, histological and physiological renal parameters. Toxicon 59 (6), 601–609. https://doi.org/10.1016/j.toxicon.2012.02.003.
Margolis, A.E., Banker, S., Pagliaccio, D., De Water, E., Curtin, P., Bonilla, A., Herbstman, J.B., Whyatt, R., Bansal, R., Sjödin, A., Milham, M.P., Peterson, B.S., Factor-Litvak, P., Horton, M.K., 2020. Functional connectivity of the reading network is associated with prenatal polybrominated diphenyl ether concentrations in a community sample of 5-year-old children: a preliminary study. Environ. Int. 134 (September 2019), 105212 https://doi.org/10.1016/j.envint.2019.105212.
Mela, M., Grötzner, S.R., Legeay, A., Mesmer-Dudons, N., Massabuau, J.C., Ventura, D.F., Oliveira Ribeiro, 2012. Morphological evidence of neurotoxicity in retina after methylmercury exposure. Neurotoxicology 33. https://doi.org/10.1016/j.neuro.2012.04.009.
Mela, M., Guiloski, I.C., Doria, H.B., Randi, M.A.F., De Oliveira Ribeiro, C.A., Pereira, L., Maraschi, A.C., Prodocimo, V., Freire, C.A., Silva de Assis, H.C., 2013. Effects of the herbicide atrazine in neotropical catfish (*Rhamdia quelen*). Ecotoxicol. Environ. Saf. 93, 13–21. https://doi.org/10.1016/j.ecoenv.2013.03.026.
Mi, X.-B., Bao, L.-J., Wu, C.-C., Wong, C.S., Zeng, E.Y., 2017. Absorption, tissue distribution, metabolism, and elimination of decabrominated diphenyl ether (BDE-209) in rats after multi-dose oral exposure. Chemosphere 186, 749–756. https://doi.org/10.1016/j.chemosphere.2017.08.049.
Montalbano, A.M., Albano, G.D., Anzalone, G., Moscato, M., Gagliardo, R., Di Sano, C., Bonanno, A., Ruggieri, S., Cibella, F., Profita, M., 2020. Cytotoxic and genotoxic effects of the flame retardants (PBDE-47, PBDE-99 and PBDE-209) in human bronchial epithelial cells. Chemosphere *245*. https://doi.org/10.1016/j.chemosphere.2019.125600.
Moustafa, E.M., Dawood, M.A.O., Assar, D.H., Omar, A.A., Elbialy, Z.I., Farrag, F.A., Shukry, M., Zayed, M.M., 2020. Modulatory effects of fenugreek seeds powder on the histopathology, oxidative status, and immune related gene expression in Nile tilapia (*Oreochromis niloticus*) infected with *Aeromonas hydrophila*. Aquaculture 515 (August 2019), 734589. https://doi.org/10.1016/j.aquaculture.2019.734589.
Nagamatsu, P.C., Rubio Vargas, D.A., Prodocimo, M.M., Opuskevitch, I., Ferreira, F.C.A. S., Zanchin, N., Oliveira Ribeiro, C.A., de Souza, C., 2020. Synthetic fish metallothionein design as a potential tool for monitoring toxic metals in water. Environmental Science and Pollution Research. ⟨https://doi.org/10.1007/s11356-020-11427-2⟩.
Oliveira Ribeiro, C.A., Bozza, D.A., Esquivel, L., DE Oliveira, E.C., Filipak, F., 2022. Comparative effects of oral exposure to 2, 4, 6-tribromophenol and decabromodiphenyl ether in Nile tilapia. Environ. Sci. Pollut. Res. 29, 17087–17102. https://doi.org/10.1007/s11356-021-16779-x.
Pardo, O., Fernández, S.F., Quijano, L., Marín, S., Villalba, P., Corpas-Burgos, F., Yusà, V., 2020. Polybrominated diphenyl ethers in foods from the Region of Valencia: dietary exposure and risk assessment. Chemosphere *250*. https://doi.org/10.1016/j.chemosphere.2020.126247.
Perussolo, M.C., Guiloski, I.C., Lirola, J.R., Fockink, D.H., Corso, C.R., Bozza, D.C., Prodocimo, V., Mela, M., Ramos, L.P., Cestari, M.M., Acco, A., Silva de Assis, H.C., 2019. Integrated biomarker response index to assess toxic effects of environmentally relevant concentrations of paracetamol in a neotropical catfish (*Rhamdia quelen*). Ecotoxicol. Environ. Saf. 182 (January), 109438 https://doi.org/10.1016/j.ecoenv.2019.109438.
Ríos, J.M., Lana, N.B., Ciocco, N.F., Covaci, A., Barrera-Oro, E., Moreira, E., Altamirano, J.C., 2017. Implications of biological factors on accumulation of persistent organic pollutants in Antarctic notothenioid fish. Ecotoxicol. Environ. Saf. 145 (February), 630–639. https://doi.org/10.1016/j.ecoenv.2017.08.009.
Rubio-Vargas, D.A., Oliveira Ribeiro, C.O., Filipak Neto, F., Cordeiro, A.L., Cestari, M.M., Câmara de Souza, A., Castro Martins, C., da Silva, C., de Campos, S.X., Esquivel, J.R., Prodocimo, M.M., 2021. Exposure to pollutants present in Iguaçu River Southern Brazil affect the health of *Oreochromis niloticus* (Linnaeus, 1758): assessment histological, genotoxic and biochemical. Environ. Toxicol. Pharmacol. 87. https://doi.org/10.1016/j.etap.2021.103682.
Salgado, L.D., Marques, A.E.M.L., Kramer, R.D., Oliveira, F.G. de, Moretto, S.L., Lima, B. A. de, Prodocimo, M.M., Cestari, M.M., Azevedo, J.C.R. de, Silva de Assis, H.C., 2019. Integrated assessment of sediment contaminant levels and biological responses in sentinel fish species *Atherinella brasiliensis* from a sub-tropical estuary in south Atlantic. Chemosphere 219, 15–27. https://doi.org/10.1016/j.chemosphere.2018.11.204.
Sanchez, W., Burgeot, T., Porcher, J.M., 2013. A novel "Integrated Biomarker Response" calculation based on reference deviation concept. Environ. Sci. Pollut. Res. 20 (5), 2721–2725. https://doi.org/10.1007/s11356-012-1359-1.
Sedlak, J., Lindsay, R.H., 1968. Estimation of total, protein-bound, and nonprotein sulfhydryl groups in tissue with Ellman's reagent. Anal. Biochem. 25 (C), 192–205. https://doi.org/10.1016/0003-2697(68)90092-4.
Serafini, S., Souza, C.F., Baldissera, M.D., Baldisserotto, B., Segat, J.C., Baretta, D., Zanella, R., da Silva, A.S., 2019. Fish exposed to water contaminated with eprinomectin show inhibition of the activities of AChE Na^{+}/K^{+}-ATPase in the brain, and changes in natural behavior. Chemosphere 223, 124–130. https://doi.org/10.1016/j.chemosphere.2019.02.026.
Sies, H., Koch, O.R., Martino, E., Boveris, A., 1979. Increased biliary glutathione disulfide release in chronically ethanol-treated rats. FEBS Lett. 103, 287–290. https://doi.org/10.1016/0014-5793(79)81346-0.
Song, Y., Miao, J., Pan, L., Wang, X., 2016. Exposure to2,2′,4,4′-tetrabromodiphenyl ether (BDE-47) alters thyroid hormone levels and thyroid hormone-regulated gene transcription in manila clam *Ruditapes philippinarum*. Chemosphere 152, 10–16. https://doi.org/10.1016/j.chemosphere.2016.02.049.
Souza, T.L., Batschauer, A.R., Brito, P.M., Oliveira Ribeiro, C.A., Martino-Andrade, A.J., Ortolani-Machado, C.F., 2019. Multigenerational analysis of the functional status of male reproductive system in mice after exposure to realistic doses of manganese. Food Chem. Toxicol. 133 (May), 110763 https://doi.org/10.1016/j.fct.2019.110763.
Souza, T.L., Batschauer, A.R., Brito, P.M., Leão-Buchir, J., Spercoski, K.M., Neto, F.F., Martino-Andrade, A.J., Ortolani-Machado, C.F., 2020. Evaluation of Mn exposure in the male reproductive system and its relationship with reproductive dysfunction in mice. Toxicology 441, 152504. https://doi.org/10.1016/j.tox.2020.152504.
Teta, C., Naik, Y.S., 2017. Vitellogenin induction and reduced fecundity in zebrafish exposed to effluents from the City of Bulawayo, Zimbabwe. Chemosphere 167, 282–290. https://doi.org/10.1016/j.chemosphere.2016.10.011.
Thornton, L.M., Path, E.M., Nystrom, G.S., Venables, B.J., Sellin Jeffries, M.K., 2016. Early Life Stage Exposure to BDE-47 Causes Adverse Effects on Reproductive Success and Sexual Differentiation in Fathead Minnows (*Pimephales promelas*). Environ. Sci. Technol. 50 (14), 7834–7841. https://doi.org/10.1021/acs.est.6b02147.
Van der Oost, R., Beyer, J., Vermeulen, N.P.E., 2003. Fish bioaccumulation and biomarkers in environmental risk assessment: a review. Environ. Toxicol. Pharmacol. 13 (2), 57–149. https://doi.org/10.1016/S1382-6689(02)00126-6.
Wendel, A., 1981. Glutathione Peroxidase. Methods in Enzymology. Academic Press, pp. 325–333.
Wolf, J.C., Wheeler, J.R., 2018. A critical review of histopathological findings associated with endocrine and non-endocrine hepatic toxicity in fish models. Aquat. Toxicol. 197 (October 2017), 60–78. https://doi.org/10.1016/j.aquatox.2018.01.013.
Wu, J.P., Wu, S.K., Tao, L., She, Y.Z., Chen, X.Y., Feng, W.L., Zeng, Y.H., Luo, X.J., Mai, B.X., 2020. Bioaccumulation characteristics of PBDEs and alternative brominated flame retardants in a wild frog-eating snake. Environ. Pollut. 258, 113661 https://doi.org/10.1016/j.envpol.2019.113661.
Xie, Z., Lu, G., Qi, P., 2014. Effects of BDE-209 and its mixtures with BDE-47 and BDE-99 on multiple biomarkers in Carassius auratus. Environ. Toxicol. Pharmacol. 38, 554–561. https://doi.org/10.1016/j.etap.2014.08.008.
Yamamoto, F.Y., Garcia, J.R.E., Kupsco, A., Oliveira Ribeiro, C.A., 2017. Vitellogenin levels and others biomarkers show evidences of endocrine disruption in fish species from Iguaçu River - Southern Brazil. Chemosphere 186, 88–99. https://doi.org/10.1016/j.chemosphere.2017.07.111.
Yamamoto, F.Y., Pereira, M.V.M., Lottermann, E., Santos, G.S., Stremel, T.R.O., Doria, H. B., Gusso-Choueri, P., Campos, S.X., Ortolani-Machado, C.F., Cestari, M.M., Neto, F. F., Azevedo, J.C.R., Ribeiro, C.A.O., 2016. Bioavailability of pollutants sets risk of exposure to biota and human population in reservoirs from Iguaçu River (Southern

Brazil). Environ. Sci. Pollut. Res. 23 (18), 18111–18128. https://doi.org/10.1007/s11356-016-6924-6.

Yang, J., Chan, K.M., 2015. Evaluation of the toxic effects of brominated compounds (BDE-47, 99, 209, TBBPA) and bisphenol a (BPA) using a zebrafish liver cell line, ZFL. Aquat. Toxicol. 159, 138–147. https://doi.org/10.1016/j.aquatox.2014.12.011.

Yu, L., Han, Z., Liu, C., 2015. A review on the effects of PBDEs on thyroid and reproduction systems in fish. Gen. Comp. Endocrinol. 219, 64–73. https://doi.org/10.1016/j.ygcen.2014.12.010.

Yuan, H., Jin, J., Bai, Y., Li, Q., Wang, Y., Hu, J., 2016. Concentrations and distributions of polybrominated diphenyl ethers and novel brominated flame retardants in tree bark and human hair from Yunnan Province, China. Chemos. Chemos. 154, 319–325. https://doi.org/10.1016/j.chemosphere.2016.03.132.

Zezza, D., Tait, S., Della Salda, L., Amorena, M., Merola, C., Perugini, M., 2019. Toxicological, gene expression and histopathological evaluations of environmentally realistic concentrations of polybrominated diphenyl ethers PBDE- 47, PBDE-99 and PBDE-209 on zebrafish embryos. Ecotoxicol. Environ. Saf. 183 (April), 109566 https://doi.org/10.1016/j.ecoenv.2019.109566.

Zhao, W., Cheng, J., Gu, J., Liu, Y., Fujimura, M., Wang, W., 2014. Assessment of neurotoxic effects and brain region distribution in rat offspring prenatally co-exposed to low doses of BDE-99 and methylmercury. Chemosphere 112, 170–176. https://doi.org/10.1016/j.chemosphere.2014.04.011.

Zhou, Z., Jian, X., Zhou, B., Lu, K., Wang, Y., 2020. Changes in the immune function of rainbow trout (*Oncorhynchus mykiss*) provide insights into strategies against BDE-47 stress. J. Hazard. Mater. 392 (January), 122212 https://doi.org/10.1016/j.jhazmat.2020.122212.

Zhu, B., Wang, Q., Wang, X., Zhou, B., 2014. Impact of co-exposure with lead and decabromodiphenyl ether (BDE-209) on thyroid function in zebrafish larvae. Aquat. Toxicol. 157, 186–195. https://doi.org/10.1016/j.aquatox.2014.10.011.